Cysteine Metabolism Regulates Pellicle Biofilm Development by Uropathogenic *Escherichia coli* and the *In Vitro* Characterization of CsgA Amyloid Formation

by

Elizabeth K. Gichana

A dissertation submitted in partial fulfillment
of the requirements for the degree of
Doctor of Philosophy
(Biophysics)
in The University of Michigan
2019

Doctoral Committee:

Professor Matthew R. Chapman, Chair
Associate Professor Julie S. Biteen
Emeritus Professor Ari Gafni
Professor Brian J. Love
Assistant Professor Kevin Wood

Elizabeth K. Gichana

egichana@umich.edu

ORCID iD: 0000-0003-3593-2329

To my parents.

ACKNOWLEDGEMENTS

I would like to thank first my advisor, Matt Chapman. He took a chance on me and allowed me, a dry lab scientist with no background in biology, to join his laboratory. His excitement and genuine joy for research and for life is infectious. He gave me the freedom to explore questions that I personally found interesting. He has helped to develop me not just into a more confident scientist but into a more confident person.

To my labmates, past and present. Matt's enthusiasm seeps into the fabric of the lab. I was welcomed into the lab warmly. Neha Jain and Maggie Evans were my two mentors. They were fantastic teachers who patiently taught me techniques and answered questions. Even after leaving the lab, they have been tremendous resources for me both in science and in life. I am thankful to them. Janet Price and I became fast friends. Her broad knowledge on even the most obscure topics still fascinates and amazes me. Her kindness and willingness to help makes everyone in the lab feel welcome. Sujeet Bhoite and I had projects that were most closely related and Sujeet was always willing to lend a hand and was a wonderful sounding board for me. Sujeet has also become a friend and I look forward to his jokes and philosophical musings. I also wanted to thank the undergraduate students with whom I have worked: Isaac Payne, Alexandra Christensen, Caitlyn Nalley, Andrew Drumheller, and Emily Bozich. Alex was always able to find any topic interesting. Isaac was able to make anything work on the first try. They were both dedicated to the lab and and to research. I feel like they taught me as much as I taught them. Cait, Andrew, and Emily helped to keep the lab functioning smoothly.

To Anthony Vecchiarelli and his lab. It's been such a pleasure to share lab space with

everyone in the lab. Anthony Vecchiarelli is a wealth of information. Pusparanee "Anne" Hakim was the first person I met in the Chapman lab. She has become one of my very good friends and has also been a huge help in my research.

To my committee members. I was grateful to have a wonderful and supportive thesis committee in Ari Gafni, Julie Biteen, Kevin Wood, and Brian Love. They gave valuable feedback and asked interesting questions which helped push my projects forward. Though Robert Bender was not on my committee, he attended our group lab meetings and provided fantastic feedback and insights into all my projects. To all of the members of the microbial supergroup. Attending these bi-weekly meetings challenged me to look at problems in new ways. I grew a lot as a scientist at these meetings.

To my collaborators in the Ruotolo and Almquivst groups for their help and expertise on the projects. To the support staff, administrators, faculty, and staff in and around MCDB and the University of Michigan that made it possible to execute all of these experiments and gain invaluable professional development. I won't be able to name everyone who helped along the way, but I want to thank you all.

My funding sources: Howard Hughes Gilliam Fellowship, Rackham Merit Fellowship, Roslyn M. Abrams Award, and the Bernard Maas Dean's Fellowship. I want to especially single out the Gilliam Fellowship for all that it did to expose to me other scientists as passionate about doing great work as they are to diversifying the professoriate. This extraordinary group of people constantly reminded me that I belonged and that I mattered. Being a part of this community was one of the best experiences of my life.

To my friends. Past and present, graduate students and "real people." I have been fortunate to meet smart, creative, funny, caring people who have become be a part of my own matrix of support. My friends have supported me through tough times but have also challenged me to grow in ways I could not have imagined.

To my brothers. They know and understand me better than anyone else. Their love and support of me and all of my goals has been the cornerstone to my success.

And finally, to my parents. My parents gave up everything and everyone that they knew and loved to bring my family to this country in pursuit of better life. It was not until I became an adult that I truly understood the gravity of that sacrifice. Words do not exist which can fully express my gratitude, but I hope that the completion of this degree will at the very least make them proud.

TABLE OF CONTENTS

LIST OF FIGURES

Figure

LIST OF TABLES

Table

ABSTRACT

Uropathogenic *Escherichia coli* (UPEC) is the major cause of urinary tract infections. These bacteria live in complex heterogenous communities called biofilms. UPEC biofilms are encapsulated in a matrix composed of proteins, exopolysaccharides, and DNA. These biofilms are responsible for a wide variety of functions including protecting the bacteria against physical and chemical stresses. The UPEC strain UTI89 produces biofilms under different environmental conditions in the lab. In static cultures UTI89 forms pellicles at the liquid-air interface and it forms wrinkled colony biofilms on solid agar plates. The major proteinaceous component of these biofilms is a functional amyloid structure called curli. This work focuses on the development of curli-dependent biofilms and developing methods of characterizing the interactions of curli with disease associated proteins.

In the first project, I established that pellicle biofilm formation can be regulated metabolically. I found that aged cultures of UPEC produced a potent pellicle biofilm inhibitor. Therefore, bacteria-free conditioned media from aged cultures of UTI89 impeded UTI89's own pellicle formation. UTI89 grown in bacteria-free conditioned media from an aged UTI89 culture exhibited deficient pellicle formation. The antibiofilm effect was dependent on cysteine metabolism. UPEC mutants in the cysteine biosynthesis pathway were able to form pellicles in conditioned media. Interestingly, cysteine metabolism mutants, including a cysE deletion strain, were able to make curli amyloids in conditioned media. The addition of exogenous cysteine restored the antibiofilm activity.

In a second project, I established a total internal reflection fluorescence microscopy assay to visualize bacterial amyloid formation in real time. The ability of curli to self-

assemble into fibril structures with nucleation dependent kinetics is a process which has primarily been investigated using bulk assays. How this fibril formation is initiated and how amyloids of one type can template the formation of amyloids of another type are questions which have been poorly studied to date. I developed a method that allows the measurement of amyloid assembly in curli and allows us to investigate the interactions between the functional amyloid curli and disease associated proteins such as alpha-synuclein at the single molecule level. This work elucidates mechanisms of biofilm regulation as well as the biophysical role that components of the biofilm play in triggering other diseases and therefore, on overall health.

CHAPTER I

Microbial Amyloids and the Extracellular Matrix

Parts of the work presented in the chapter are derived from work in preparation to be submitted as a review article to mBio.

Gichana, E.K., Chapman, M.R.

1.1 Introduction

Escherichia coli (*E. coli*) is a rod-shaped, Gram-negative bacterium classified as a member of the family *Enterobacteriaceae* within the Gammaproteobacteria class. It is closely related to such well known pathogens as *Salmonella, Klebsiella, Serratia*, and *Yersinia pestis* (Brenner and Farmer, 2007). *E. coli* is one of the most studied and understood organisms is science. What makes it an ideal model organism is that it is fast growing, versatile and can be found in a variety of environments and conditions. *E. coli* can even be found in environmental wastewater where it is used as a fecal indicator bacterium to indicate contamination [74]. The *E. coli* genome contains about 4,800 genes, 1700 of which are shared amongst all *E. coli* strains [77].

However, *E. coli* is also part of the commensal flora of many animals including humans. *E. coli* can also be an important pathogen. While some bacteria are restricted to specific niches within the host, *E. coli* can colonize and cause infection in a variety of sites. These

include the urinary tract, respiratory system, skin, soft tissue, and the gastrointestinal tract [18].

Within a human host, *E. coli* is most commonly found in the lower intestinal tract. The gut microbiome is dominated by obligate anaerobes (90%), as it is an anoxic environment [11]. *E. coli*, a facultative aerobe is the most common of the aerobes, but only makes up up to about 5% of the constitution [18]. *E. coli* makes its home in the thin layer of mucus that lines the gut where it grows in a multi-species biofilm [14] meaning that it is in constant competition for nutrients and or survival. Because of its location in the lower intestinal tract, *E. coli* is often found in feces which are then excreted from the host, meaning that *E. coli* can end up in places like wastewater and in the soil and has been shown to survive for long periods of time [74]. These environments are completely different than of the host in terms of the types of nutrients that are available, availability to oxygen, temperature, and the competitors.

This ability of *E. coli* to survive in a variety of areas can lead to disease. As an example, urinary tract infections are some of the most common bacterial infections. And although many different species of bacteria can cause these infections, 80% of infections are caused by uropathogenic strains of *E. coli* [129]. The proximity of the urethral opening to the rectum makes it possible for bacteria to make it into the urethra and up to the bladder [49]. Once in the bladder, UPEC invade the bladder epithelial cells where they form biofilms to allow themselves to evade the host‘s immune system responses and drugs [155].

1.2 Biofilms

Many bacteria, including *E. coli* live as members of complex communities called biofilms [46, 61]. Bacteria living within biofilms are encapsulated in an extracellular matrix composed of proteins, exo-polysaccharides, and DNA. These biofilms are responsible for a wide variety of functions including; protecting the bacteria against physical and chemical stresses such as oxidative stress and dessication [20, 61]. Biofilms also help bacteria

to evade the host‘s immune responses and reduces the ability of antimicrobial agents to combat things like infections [3, 54, 66, 107].

Within biofilms, we see distinct populations of cells and extracellular matrix production is restricted to a distinct subpopulation [36, 41, 70, 124]. Factors which control the expression of the matrix components include temperature, osmolarity, oxygen, and nutrient availability [53, 53, 92, 100]. In the lab, bacteria form biofilms in low salt, low temperature, and low nutrient conditions [42, 62].

In *E. coli* and *Salmonella enterica* biofilms, the major protein component are aggregative fibers known as curli, which constitutes 85% of the matrix composition, and the major polysaccharide component is the carbohydrate polymer cellulose which constitutes the majority of the remaining 15% [23, 115, 163]. The expression of curli and cellulose relies on the master biofilm regulator CsgD [62, 98, 110]. The expression of CsgD is complex and relies on small RNAs, regulatory networks, environmental cues, posttranslational phosphorylation, and many transcriptional regulators [42]. This complex regulation gives rise to precision control of curli and cellulose production. Disregulation of CsgD can result in altered biofilm phenotypes.

For instance, some strains of bacteria have been found to form biofilms at elevated temperatures [36, 119]. From these studies, it was discovered that cysteine homeostatis impacts biofilm formation and the production of extracellular matrix components as well as the folding and stability of entracytoplasmic proteins [70]. CsgD is a trasncriptional regulator of *adrA*, which encodes for a diguanylate cyclase which produces a secondary messenger, cyclic-di-GMP (c-di-GMP) [163]. ci-di-GMP binds to the cellulose synthase BcsA, leading to its activation [101, 163]. CsgD requires c-di-GMP from to proteins YfiN amd YfiM [69, 150]. YfiN is inhibited by the redox-sensitive regulator YfiR. As YfiR is depleted, YfiN dimerizes and leads to unregulated cellulose production [69]. This shows that cysteine auxotrophs have increased curli and decreased cellulose production. This is due to a cellulose and curli production are tightly coupled and mediated by the cysteine

biosynthesis gene *cysE* [70].

1.3 Modeling biofilms in the laboratory

Models of the biofilm can be grown in the lab to help investigate environmental, molecular and genetic factors modulating biofilms formation. *E. coli* forms two types of biofilms in the laboratory. When grown in glass culture tubes or polystyrene tissue culture plates in static liquid cultures, *E. coli* forms a floating biofilms at the air liquid interface called pellicles (Figure 1.1A) [72, 76]. Pellicles are composed of cells encased in a matrix of curli and cellulose. Pellicle formation can then be quantified by crystal violet staining of the biomass [160]. Pellicle biofilm production is reliant on CsgD which regulates the expression of the matrix components [42]. These pellicle biofilms can be inhibited by the presence of glucose, high osmolarity, and temperatures greater than 30°C [59, 100].

Under the right conditions, *E. coli* can also produce wrinkled colony biofilms on solid agar plates which spread away from the initial site of inoculation (Figure 1.1B) [36]. Many bacteria including *E. coli, Salmonella spp., Citrobacter koseri, Psudomonas aeruginosa, and Bacillus subtilis* can form these types of biofilms [20, 36, 112, 119]. These wrinkles go by many names depending on the strain. They are sometimes called rdar (red, dry, and rough), rugose, or wrinkled colony biofilms, though for this work, we stick to rugose to refer to these types of biofilms [22, 36]. Within the rugose biofilms, matrix production also takes place at the air-colony interface where the oxygen exposed cells express matrix components [36]. The phenotype can be analyzed by growing the biofilm on plates supplemented with Congo red [160]. The development of rugose and pellicle biofilms requires expression of curli and cellulose [36, 76, 162]. Both curli and cellulose bind Congo red dye which leads to colonies red in color, indicating curli only or curli and cellulose production. It can lead to colonies pink in color, which indicates cellulose only production. If both curli and cellulose production is affected, as with the deletion of csgD (Figure 1.1B) rugose colonies spread less, have a smaller diameter, and do not bind the dye [119, 163].

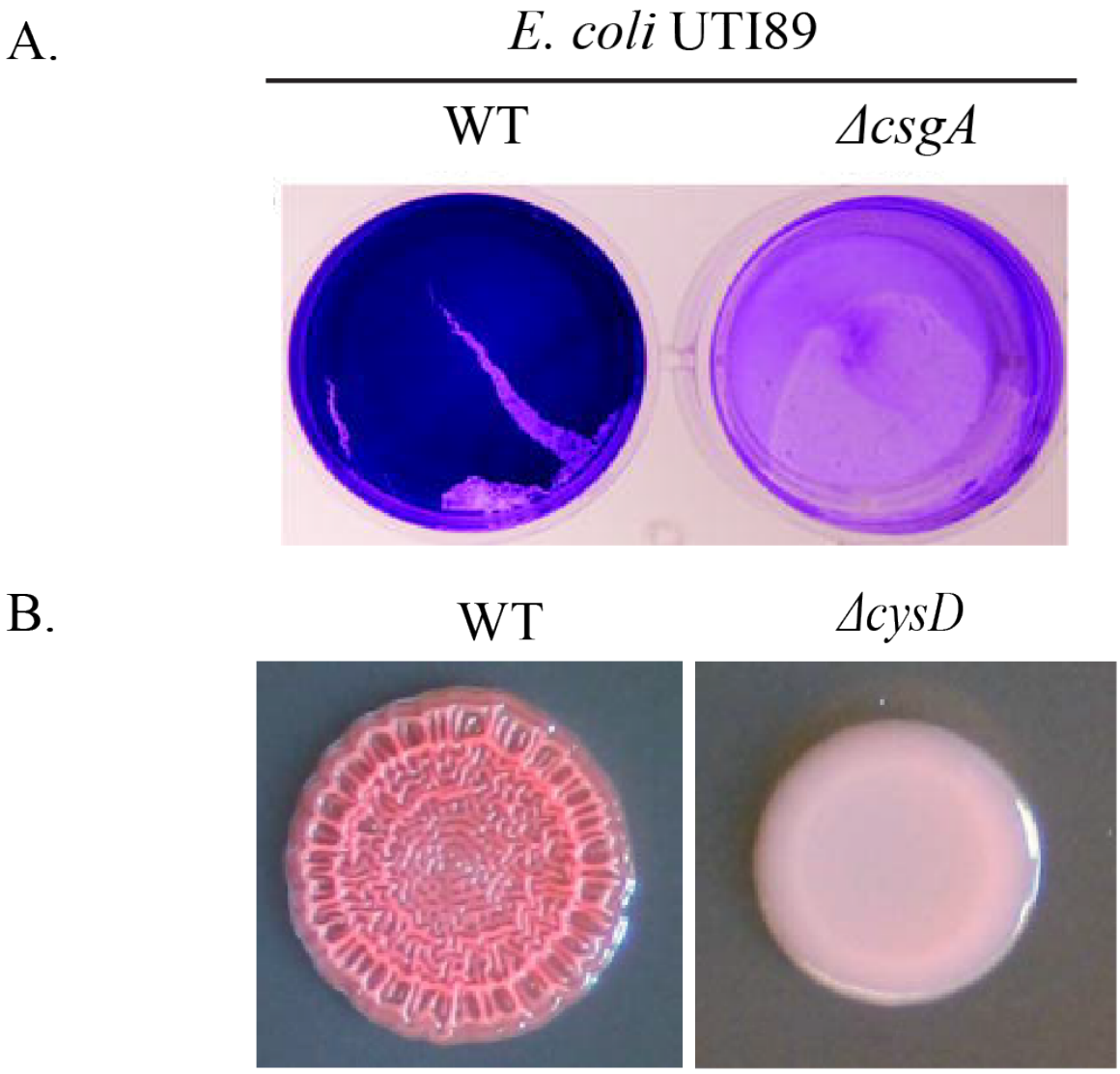

Figure 1.1: Modeling biofilms in the laboratory. (A.) WT UTI89 grown in static culture at 26 °C forms a pellicle biofilm in a microtiter plate. The planktonic cells have been removed and the pellicle was stained with 0.1% crystal violet. A UTI89 Δ*csgA* mutant is unable to form a pellicle under these same conditions [160]. **(B.)** Rugose biofilms form complex spreading and wrinkling patterns which are dependent on the master biofilm regulator CsgD. UTI89 Δ*csgD* mutant colonies do not spread as much as WT, do not wrinkle, and do not bind Congo red dye. Figure reproduced from [71, 160].

1.4 Microbial amyloids

Amyloids are most famous because of their implication in diseases such as Alzheimers and Parkinsons Disease (Cooper et al., PNAS 1987; Glenner et al, Biochem Biophys Res Comm. 1984; Steffan et al PNAS 2000; Pruisner et al Trends Biochem Sci 1996; Chiti and Dobson Annu Rev Biochem 2006). In fact, amyloids are now associated with 36 human diseases. These range from systemetic diseases such as renal amyloidosis, the well-known neurodegenerative diseases, and even prostate cancer [28].

A class of amyloids, termed functional amyloids, exists that stands independently of disease associated amyloids. These structures are not the result of protein misfolding, but are rather are the product of highly regulated assembly and serve important roles in cell physiology. Functional amyloids are now found in all kingdoms of life. They are found in fungi, mammals, and bacteria [**?**, 16, 17, 23, 40, 48, 136]. Microbial amyloids are by far the largest class of functional amyloids. Microbial amyloids are responsible for a wide variety of functions including; biofilm formation, adhesion, invasion of host cells, host pathogen interactions, as well as regulating inflammatory and immune responses in the gut [1, 8, 52, 56, 57, 75, 85, 104, 114, 118, 138, 139, 144].

Despite their varied sequence composition, sizes, and biological functions, currently, amyloid fibrils are biophysically characterized by their repeating cross-β-sheet architecture when examined by x-ray diffraction. The subunits are oriented perpendicular to the fiber axis and stabilized by hydrogen bonds between backbone amide groups [39, 132]. These structures are highly stable, resistant to proteolytic degradation and SDS, and they bind to amyloids specific dyes such as Congo red and ThT. Figure reproduced from [39,96].

1.4.1 Curli

Curli are among the best-studied of the microbial amyloids. Curli are an integral part of the biofilm extracellular matrix produced by *Salmonella, Enterobacteriaceae*, and *E. coli* (Chapman et al, Science 2002; Collinson et al J Bac 1993; Solomon et al J food Prot 2005;

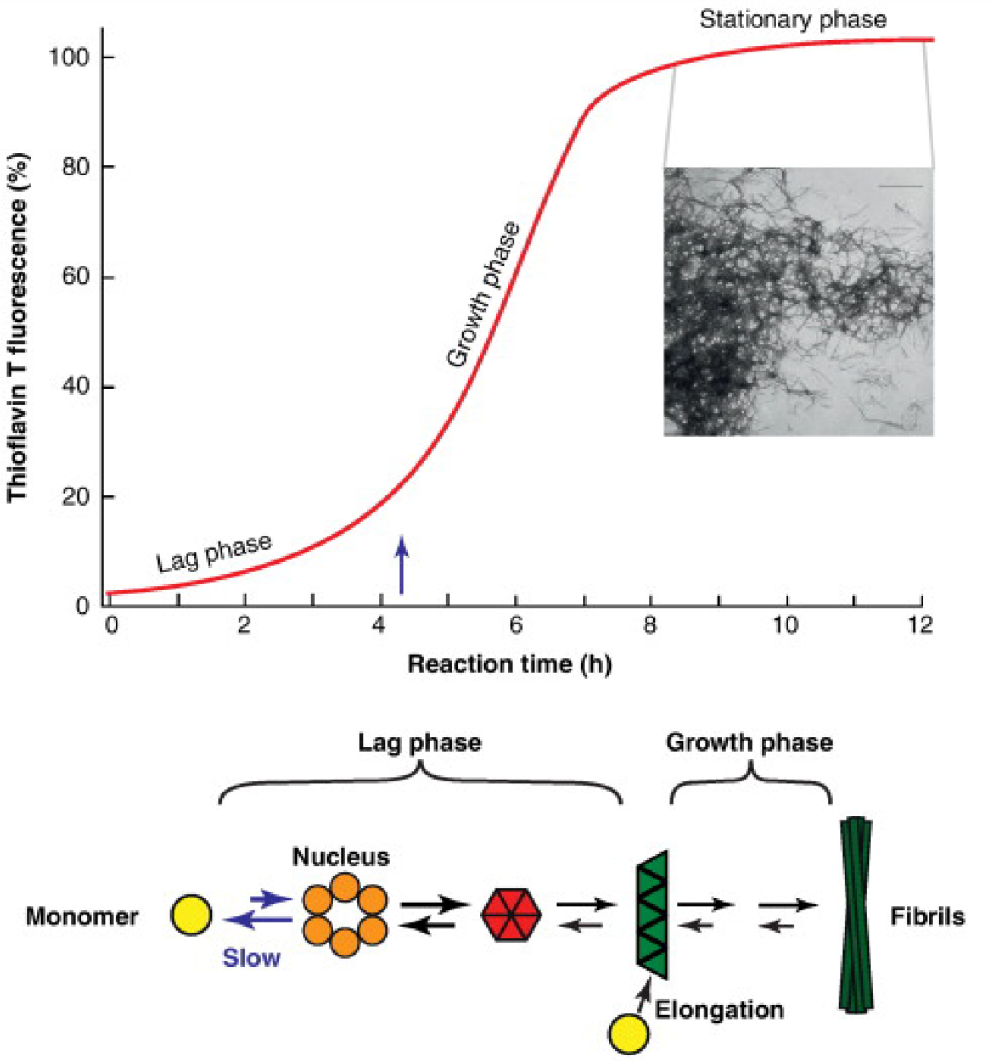

Figure 1.2: In vitro polymerization of amyloids. This schematic illustrates protein monomers polymerizing into amyloid. The lag phase, growth phase, and stationary phases are indicated. The blue arrow indicates the end of the lag phase. Figure reproduced from reference [17].

Hung et al, MBio 2013).

Curli fibers are composed of heteropolymeric fibrils CsgA, the major curli subunit, and CsgB, the minor curli subunit. Though the structure of these fibrils has not yet determined at the molecular level, must of the structural data that does exist, the results of X-ray diffraction, electron microscopy, NMR, and other fluorometric methods, suggests that these fibers have stacked β-helical subunits rather than an in-register β-sheet structure found in disease associated amyloids [125, 135]. All the same, these fibrils display all of the same structural and biophysical properties as disease associated amyloids [23].

Unlike disease associated amyloids which are thought to be the result of protein misfolding (REF), these functional amyloids are the product of a highly coordinated biosynthetic pathway [17, 141].

Curli are the result of two divergently transcribed operons, csgBAC and csgDEFG [23, 62]. Curli subunits are assembled in what is known as type VIII secretion [15, 141] (Figure 1.2).

As mentioned previously, expression of curli is also controlled by several environmental signals, but curli are primarily expressed during stationary phase and at low temperatures (REFs). There are a few mutants and clinical isolates that have been shown to express curli at higher temperatures (REFs). Transcription of the *csgBAC* operon is internally regulated by CsgD, the first gene product of the csgDEFG operon [162](Zogaj et al., 2003; Dudin et al., 2014). CsgD activates the transcription of *csgBAC*. CsgA is the primary structural element of the curli fiber. It has a core amyloid region made up of 5 imperfect repeat units with a conserved consensus sequence made up of arginine and glutamine residues [26, 148]. The arrangement of the repeats aligns the glutamine and asparagine residues which stack up and stabilize the fold. The internal repeats, R2-R4, contain a critical set of residues termed “gatekeepers” which modulate amyloid formation. The terminal repeats R1 and R5 are responsible for interactions with the minor subunit protein, CsgB [148, 149](Wang and Chapman, J Biol Chem 2008; Wang et al., PNAS 2010).

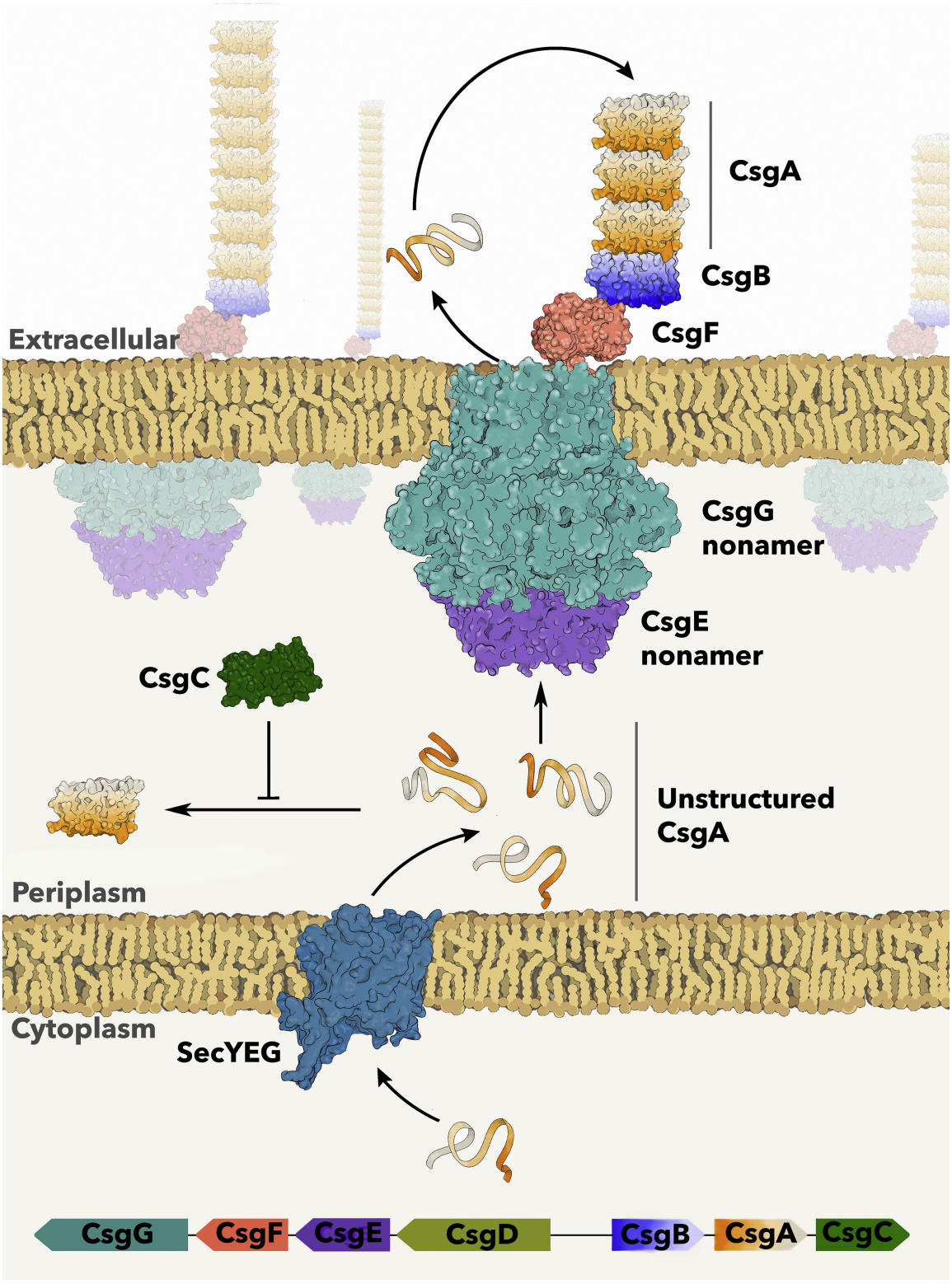

Figure 1.3: Curli biogenesis - working model. The *csg* operon encodes the curli specific genes. CsgA, the major curli subunit, is transported into the periplasm by the SecYEG translocon. CsgA is kept soluble by CsgC until it can be delivered to CsgG by the accessory protein CsgE for secretion. CsgA is nucleated into ordered amyloid fibers on the cell surface by CsgB in a CsgF dependant manner [37].

CsgB is responsible for nucleating CsgA into a curli fiber. CsgA and CsgB sequences are about 30% identical. It also has a core amyloid region made up of five strands. The first four repeats share the same motif as CsgA‘s R1-R4, but R5 is unique [64, 65](Hammer et al., PNAS 2007; Hammer et al., J Mol Biol 2012). Truncation of this strand still results in an amyloidogenic protein that can nucleate and polymerize CsgA. CsgB adheres to the cell wall at the c-terminus and exposes a template for recognition by an R1 or R5 repeat of a CsgA. CsgF helps to tether CsgB to the cell wall [97] (Nenninger et al., PNAS 2009). Addition of CsgF to CsgB in vitro considerably speeds up aggregation of CsgB, and in fact, seems to help CsgB adopt a proper amyloid fold.

CsgA and CsgB are secreted through an outer membrane lipoprotein, CsgG [89,117](Loferer et al., Mol Microbiol 1997; Robinson et al., Mol Micro 2006). CsgA and CsgB are targeted to CsgG by a 22-amino acid N-terminal signal sequence [117](Robinson et al., Mol Micro 2006). CsgG is complex of 9 identical subunits. Each subunit has four β-strand subunits which assemble to form a β-barrel with 36 transmembrane β-strands [21, 58](Goyal et al, Nature 2014; Cao et al., PNAS 2014). Each of these units also contributes 3 residues to a series of rings that constrict the secretion channel to a diameter of 9A and function as gatekeepers for the selective secretion of the unstructured curli subunits [21](Cao et al., PNAS 2014). CsgG is aided by CsgE, another periplasmic protein that assembles as a nonameric cap to CsgG that traps CsgA in the periplasmic vestibule of CsgG, facilitating CsgA’s translocation to the outter membrane [80](Klein et al., MBio 2018).

CsgC, a periplasmic accessory protein, inhibits amyloid fibril formation within the periplasm (Evans et al., Mol Cell 2015). It does this by inhibiting primary nucleation or elongation via a series of electrostatic interactions [126, 133, 134].

1.5 Modulation of amyloid fibril formation

Because of the role that amyloids play in causing such devastating human diseases as Alzheimer‘s and Parkinson‘s disease, much effort has been exerted at identifying chemi-

cals that are able to prevent their formation. *E. coli* and its highly regulated curli biogenesis system represents an elegant model along with a suite of tools with which to screen for molecules which are able to modulate the amyloid formation.

The Chapman lab has been screening and characterizing a library of designer peptidomimetic compounds called 2-pyridones. These compounds were initially recognized as anti-amyloid in a screen of small molecule molecules in testing for their efficacy in binding to Aβ-42, an amyloid associated with Alzheimer's disease [6, 22, 67, 83]. One of the 2-pyridone compounds, FN075, proved to be a potent amyloid inhibitor. It inhibits Aβ and CsgA polymerization in vitro and blocks curli biofilm formation in biofilm assays. In a UTI89 mouse model, FN075 resulted in decreases in intracellular bacterial communities [22]. FN075 was also tested against another amyloid protein, α-synuclein, which associated with Parkinson's disease. Interestingly, FN075 accelerated α-synuclein fibril formation [67].

Curli have also been shown to trigger α-synuclein aggregation [24]. The process by which these two proteins interact to promote amyloid formation is known as cross-seeding [102]. Considering that many amyloids share structural and kinetic characteristics, it makes intuitive sense that there would be molecular cross-talk.

1.6 Dissertation Goals

The aims of this dissertation are to identify inhibitors of biofilm formation as well as investigate the mode by which the known inhibitor FN075 and the human disease associated amyloid α-synuclein modulate amyloid formation. In chapter 2 I find that *E. coli* UTI89 conditioned media is able to inhibit its own growth by an effect that is dependent on cysteine metabolism. In chapter 3, I develop a real-time fluorescence microscopy assay that will allow us to characterize interactions between amyloid proteins and proteins and chemical modulators. In chapter 4, I characterize the effects of small molecules on the polymerization of CsgA.

CHAPTER II

Conditioned Media of Uropathogenic *E. coli* Impede Its Own Biofilm Development *via* Cysteine Metabolism

The work presented in this chapter is in preparation for publication.

Gichana, E.K.*, Zhou, Y.*, Hung, C., Leong, B.J., Hultgren, S.J., Chapman, M.R.

[1]Conditioned Media of Uropathogenic *E. Coli* Impede Its Own Biofilm Development via Cysteine Metabolism.

2.1 Introduction

Many bacteria live as members of complex communities called biofilms [33, 60, 106]. Bacteria living within biofilms are encased in an extracellular matrix composed of proteins, exopolysaccharides, and extraxellular DNA [79]. Biofilms are linked with a variety of chronic infections and have increased resistance to antimicrobial agents and environmental stress [4,5,88,91]. *Eschericia coli*(*E. coli*) is a major cause of urinary tract infections. A clinical uropathogenic *E. coli* (UPEC) isolate UTI89, forms biofilm-like intracellular communities in bladder epithelium cells which protect UPEC from immune clearance [22,103].

[1]**Author contributions** - E.K.G. and Y.Z. contributed equally to this work.

In a laboratory setting, UTI89 develops rugose colony biofilms on solid agar surfaces and pellicle biofilms floating at the air-liquid interface of static cultures [72, 76]. The development of colony and pellicle biofilms requires expression of curli and cellulose [36, 76, 162]. Curli are functional amyloid fibers produced on the surface of many enteric bacteria [111]. Curli fibers are both adhesive and stable which makes them perfect structures for facilitating both bacteria-surface and bacteria-bacteria interactions [119]. The expression of both curli and cellulose is controlled by the master regulator CsgD [19, 120, 163].

Many bacteria are capable of producing metabolic intermediates or structural components that prevent their own biofilm formation or inhibit biofilm development of other species [63, 81, 86, 116, 140, 146]. For instance *Staphylococcus aureas* exports cyclic autoinducing peptides to the environment, which triggers biofilm dispersion via the accessory gene regulator (agr) system [81]. *Bacillus subtilis* releases D-amino acids as the cultures ages, which not only disperse its own pellicle biofilm, but can also prevent biofilm formation of a broad spectrum of bacteria species [81, 140]. the gram-negative bacterium *Vibrio cholerae* utilizes quorum sensing molecules to repress biofiom matrix production at high cell density [25, 161]. In *E. coli*, self-produced indole and capsular polysaccharides also exhibit antibiofilm activity [86, 140, 146]. O-acetylated serine (OAS) has also been implicated as in inhibitor of *E. coli* biofilms [131]. OAS is produced from serine by serine acetyltransferase, CysE. OAS is then converted to cysteine by two functionally redundant OAS sulfhydrylases, CysK and CysM.

In this study we found aged biofilm cultures of UTI89 demonstrated antibiofim activity against its own pellicle formation. The potential biofilm inhibitor is heat-stable and is resistant to protease treatment. A candidate approach revealed that the antibiofilm activity of the conditioned medium is dependent on cysteine metabolism, as conditioned media of cysteine auxotrophs Δ*cysE* and Δ*cysK*Δ*cysM* lost the antibiofilm activity. Cysteine metabolism also controls biofilm architecture of UTI89 pellicle and rugose biofilm.

2.2 Experimental Procedures

2.2.1 Bacterial Strains, Media, and Growth Conditions

The well-characterized uropathogenic *E. coli* isolate UTI89 was provided by Scott Hultgren [32, 94]. UTI89 mutants were generated by red-swap as described [151] or kindly provided by the Hutgren lab. These mutants are listed in Table 2.1. Primers used to construct these mutants are listed in Table 2.2. Unless otherwise stated, bacteria were typically grown in LB at 37°C with shaking.

Table 2.1: Strains used in this study

Bacterial strains	Relevant genotype and features	Resistances	References
Wild-type UTI89	Wild-type clinical UPEC	None	[94]
UTI89 Δ*csgA*	Deletion of the major culrlin gene, *csgA*, in UTI89, abolishment of curli expression	None	[22]
UTI89 Δ*cysE*	Deletion of the serine acetyltransferase *cysE*	None	[70]
UTI89 Δ*cysK*Δ*cysM*	Deletion of cysteine synthases *cysK* and *cysM*	None	[70]
UTI89 Δ*csgBA*	Deletion of the curli operon *csgBA*	None	[36]
UTI89 Δ*csgD*	Deletion of the curli and cellulose regulator *csgD*	None	[36]
UTI89 Δ*tnaA*	Deletion of the tryptophanase *tnaA*	None	This study
UTI89 Δ*gshA*	Deletion of the γ-glutamate-cysteine ligase *gshA*	Kanamycin	This study
UTI89 Δ*gshB*	Deletion of the glutathione synthase *gshB*	Kanamycin	This study
UTI89 Δ*kpsS*	Deletion of the polysialic acid capsule synthesis gene *kpsS*	None	From the Hultgren lab
UTI89 Δ*kpsF*	Deletion of the polysialic acid capsule synthesis gene *kpsF*	None	From the Hultgren lab

2.2.2 Pellicle biofilms

Pellicle biofilms of UTI89 were cultivated as previously described [160]. Overnight cultures of UTI89 grown in LB were diluted 1:1,000-fold into 2mL of YESCA media (1%

Primer	Primer Sequence	Constructs
Cyse rsF	5’-GCCCGCGCAGAACGGGTCGGTCATTATCTTA TCGTGTGGAGTAAGCAATGCATATGAATATCCTCCTTAG -3’	UTI89 *ΔcysE*
cysersR	5’- CACGCCGCATCCGGCACGATCACAGAATG TCAGATCCCATCACCATACTCGTGTAGGCTGGAGCTGCTTC-3’	UTI89 *ΔcysE*
csymrsf	5’-AGACGCGTAAGCGTCGCATCAGGCAACACC ACGTATGGACAGAGATCGTGGTGTAGGCTGGAGCTGCTTC -3’	UTI89 *ΔcysKΔcysM*
cysmrsr	5’-ACGGATAAAACGGTGCCTGCGCAATAATCT TAAATCCCCGCCCCCTGGCTCATATGAATATCCTCCTTAG -3’	UTI89 *ΔcysKΔcysM*
cyskrsf	5’-GGTATGCTACCTGTTGTATCCCAATTTCATA CAGTTAAGGACAGGCCATGGTGTAGGCTGGAGCTGCTT-3’	UTI89 *ΔcysKΔcysM*
cyskrsf	5’-CTTTTTTACGCATTTTTTACAAGCTGGCATT ACTGTTGCAGTTCTTTCTCCATATGAATATCCTCCTTAG -3’	UTI89 *ΔcysKΔcysM*
csgD RS	5’-CAATCCAGCGTAAATAACGTTTCATGGCTTT ATCGCCTGAGGTTATCGTTCATATGAATATCCTCCTTA-3’	UTI89 *ΔcsgD*
csgD RS	5’-GAGGCAGCTGTCAGGTGTGCGATCAATAAA AAAAGCGGGGTTTCATCATGGTGTAGGCTGGAGCTGCTTC-3’	UTI89 *ΔcsgD*
csgD RS seq	5’-TGTAATGGCTAGATTGAAATCAGATG-3’	UTI89 *ΔcsgD*
csgD RS seq	5’-TGGGCCTTTCATTAATCGTT-3’	UTI89 *ΔcsgD*
csgBA RS	5’-AAATACAGGTTGCGTTAACAACCAAGTTGA AATGATTTAATTTCTTAAGTGTGTAGGCTGGAGCTGCTT-3’	UTI89 *ΔcsgBA*
csgBA RS	5’-CGAAAAAAAACAGGGCTTGCGCCCTGTTTC TTTAATACAGAGGATGTATATGAATATCCTCCTTAG-3’	UTI89 *ΔcsgBA*
csgBA seq	5’-CGCAGACATACTTTCCATCG-3’	UTI89 *ΔcsgBA*
csgBA seq	5’-GAAAGTGCCGCAAGGAGTAA-3’	UTI89 *ΔcsgBA*
tnaA rs	5’-AATATTCACAGGGATCACTGTAATTAAAAT AAATGAAGGATTATGTAATGGTGTAGGCTGGAGCTGCTTC-3’	UTI89 *ΔtnaA*
tnaA rs	5’-ACATCCTTATAGCCACTCTGAGTGTTTTAAT TAAACTTCTTTCAGTTTTGCCATATGAATATCCTCCTTAG-3’	UTI89 *ΔtnaA*

Figure 2.1: Primers used in this study.

casamino acid and 0.12% yeast extract) or 1mL of fresh YESCA media mixed with conditioned media in wells of 24-well tissue culture plates. Bacterial cultures were incubated statically at 26°C for 32-48 hours before analyeses were performed. For better visualization, each well was stained with 2mL of 0.1% crystal violet and washed with PBS twice. To prepare conditioned media, overnight cultures of UTI89 was diluted by 1:1,000-fold into 4-6mL YESCA media in glass culture tubes and incubated statically at 26°C for 4-5 days. Bacteria-free conditioned media was made by passing the 4 day old cultures through a 0.2mm syringe filter and stored at 4°C for no longer than 2 weeks.

2.2.3 Rugose colony biofilms

Rugose biofilms were grown as previously described [36]. Briefly, overnight cultures of WT UTI89 or mutant strains grown in LB were normalized to an OD_{600} of 1 and 4µL of the normalized culture was spotted onto YESCA agar. For complementation assays with exogenous cysteine or o-acetyl-serine (OAS), sterile paper discs with 10% (m/v) cysteine or OAS were placed 2 cm away from freshly spotted bacteria on YESCA agar. Bacteria were incubated at 26°C for 48 hours.

2.2.4 Colony forming units (CFU) measurements of rugose biofilm

WT UTI89 and Δ*cysE* rugose colonies grown on YESCA and YESCA supplemented with 25µM of cysteine for 48 hours. Colonies were resuspended in 1mL of 50mM potassium phosphate buffer pH 7.2 and tissue homogenized prior to serial dilution and CFU determination.

2.2.5 Western blot analysis

To determine protein expression in UTI89 grown in conditioned media or the fresh medium, bacteria grown at 26°C for 24 hours were collected, including biofilm cells and planktonic cells. Collected bacteria were homogoenized for 20 seconds to separate bacteria

in the pellicle. Bacterial cell densities of homogenized cultures were normalized based on optical density at 600nm.

Western blot analysis of CsgA was performed as previously described [151]. Briefly, normalized bacteria pellets from pellicle cultures or colony biofilms were treated with or without 70μL HFIP. HFIP treated samples were then dried immediately in a SpeedVac at 45°C for 35 mins. Both HFIP treated and non-treated samples were resuspended directly in 150μL 2X SDS loading buffer. Non-HFIP treated samples were also used for detection of CsgD. Samples were loaded onto 15% SDS-PAGE gels. To detect CsgA, proteins were transferred onto a PVDF membrane by semi-dry transfer and probed with rabbit anti-CsgA serum (Proteintech Group, Inc., Chicago, IL). For CsgD and RpoS, wet-transfer was carried out and blots were probed with rabbit anti-CsgD serum (kindly provided by Dr. Ute Rombling) or by anti-RpoS antibody (Santa Cruz Biotechnology, Inc.) [65].

2.2.6 Growth curve measurements

UTI89 wild-type or mutants were inoculated in LB medium at 37°C overnight and diluted by 1:1,000 fold into 200μL YESCA, YESCA mixed with H2O, or YESCA mixed with the conditioned medium in wells on 96-well microtiter plate. The plate was sealed with transparent sticker. OD_{600} was measured by a plate reader (Molecular Devices, Sunnydale, CA) every hour in a 48 hour period of time. The fresh YESCA medium with no bacteria was used as the control.

2.3 Results

2.3.1 Conditioned UTI89 cultures impedes its own biofilm formation

UTI89 forms robust pellicle after 2-3 days of incubation in static liquid YESCA at 26°C [72]. To investigate if UTI89 produces antibiofilm molecules during growth, we collected filter-sterilzed UTI89 biofilm culture media after biofilms had grown at 26°C for 3-5 days.

Conditioned media were mixed with fresh YESCA media at a 1:1 (v/v) ratio which was then used in pellicle biofilm assays. A deficient biofilm formation phenotype was observed for UTI89 grown in conditioned media (Figure 2.1A). UTI89 was only able to form a thin, fragile pellicle in conditioned media collected from 3 day old cultures and was unable to form a pellicle in conditioned media collected from 4 and 5 day old cultures after 48 hours of incubation (Figure 2.1A). As a control, UTI89 formed robust pellicles in fresh YESCA or fresh YESCA mixed 1:1 (v/v) with H2O, indicating that the deficient pellicle formation in conditioned media is not due to nutrient limitation (Figure 2.1A; also mention the supplementation of nutrients to the spent media). Additionally, no substantial growth defects were observed for UTI89 grown in the conditioned medium in comparison to that in the fresh medium or diluted fresh medium (Figure 2.1B).

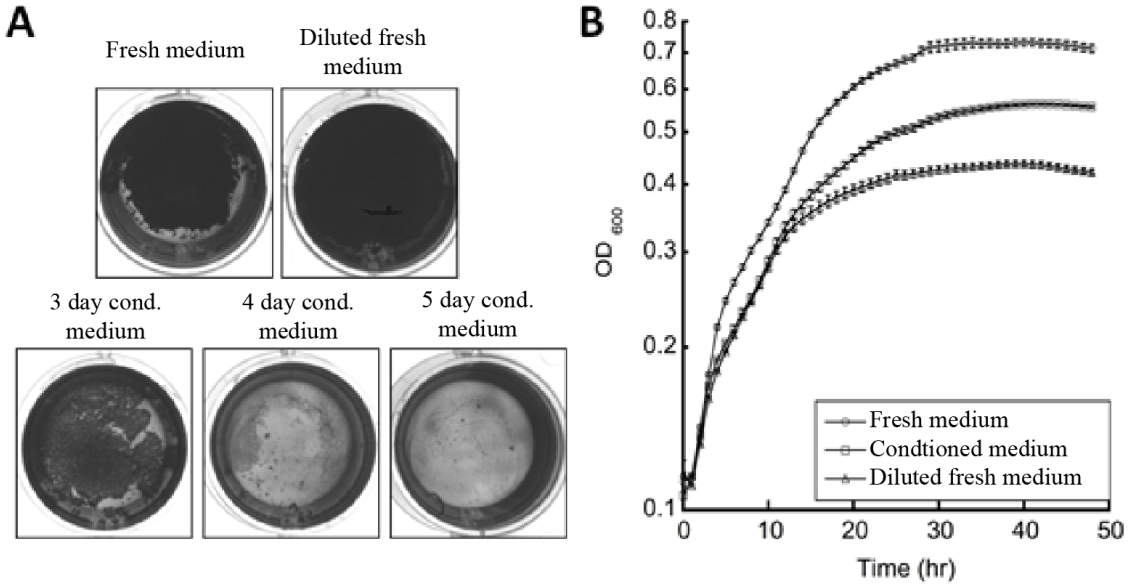

Figure 2.2: Conditioned media collected from UTI89 cultures impeded its own pellicle formation. (A) UTI89 was grown statistically at 26°C in the fresh YESCA medium, the diluted fresh medium, or conditioned media collected from 3-5 day old cultures. Bacteria were grown on a 24-well tissue culture plate for 48 hours. Each well was stained with crystal violet for a better visualization. **(B)** Growth curves of UTI89 in the fresh YESCA medium (circle), the conditioned medium (square), and the diluted fresh medium (triangle) on a 96-well plate. Bacteria were grown at 26°C statistically for 48 hours. Optical density was measured at 600nm by a plate reader. Each experiment was measured with 6 replicates.

The biofilm-deficient phenotype is not caused by an increase of pH from 6.6 in fresh YESCA to 8.1 in conditioned media, as fresh media at pH 8.1 still supported robust pellicle

formation (Figure 2.2A). Consistent with this result, UTI89 was unable to form a pellicle in the conditioned medium buffered to pH 6.6 (Figure 2.2A). Further characterization revealed that conditioned media was resistant to extended boiling at 95°C or proteinase K treatment (Figure 2.2B), indicating potential antibiofilm factor is not likely a protein. It is, however, still possible that polysaccharides or heat-stable small molecules are the antibiofilm factor. It is possible that the antibiofilm agent was trapped by the cellulose membrane or lost activity. Moreover, conditioned media collected from pellicle defective mutants Δ*csgD* and Δ*csgBA* maintained the pellicle inhibitory effects (Figure 2.2C), suggesting the antibiofilm factor is predominantly derived from the planktonic culture.

2.3.2 Candidate approach unveils cysteine metabolism as responsible for the antibiofilm activity

In order to identify the potential antibiofilm component in the conditioned medium, a candidate approach was utilized. We determined that the common biofilm inhibitors – indole, capsular polysaccharide, D-amino acids, and norspermidine, were not responsible for this antibiofilm activity (Figure A2). Cysteine and the precursor OAS have been shown to modestly inhibit biofilm formation of *S. aureus* and *E. coli* MG1655 [131, 156]. Interestingly, conditioned media harvested from UTI89 cysteine auxotroph mutants Δ*cysE* and Δ*cysK*Δ*cysM*, supported pellicle formation of UTI89 (Figure 2.3B). CysE is a serine acetyltransferase that conversts serine to OAS [82]. The OAS sulfhydrylases CysK and CysM further convert OAS to cysteine (Figure 2.3A) [10,47,158]. Restoration of pellicle formation in conditioned media from Δ*cysE* and Δ*cysK*Δ*cysM* mutants was not due to an increase of bacterial growth or higher cell density, as the growth rate of UTI89 in the Δ*cysE* conditioned media was almost identical to that in the wild-type conditioned medium (Figure A3). The antibiofilm effect was restored by expressing Δ*cysE* or Δ*cysK* in trans from a plasmid in a Δ*cysE* mutant or a Δ*cysK*Δ*cysM* mutant, respectively (Figure 2.3C).

To investigate if the antibiofilm activity of the conditioned media is cysteine-depenedent,

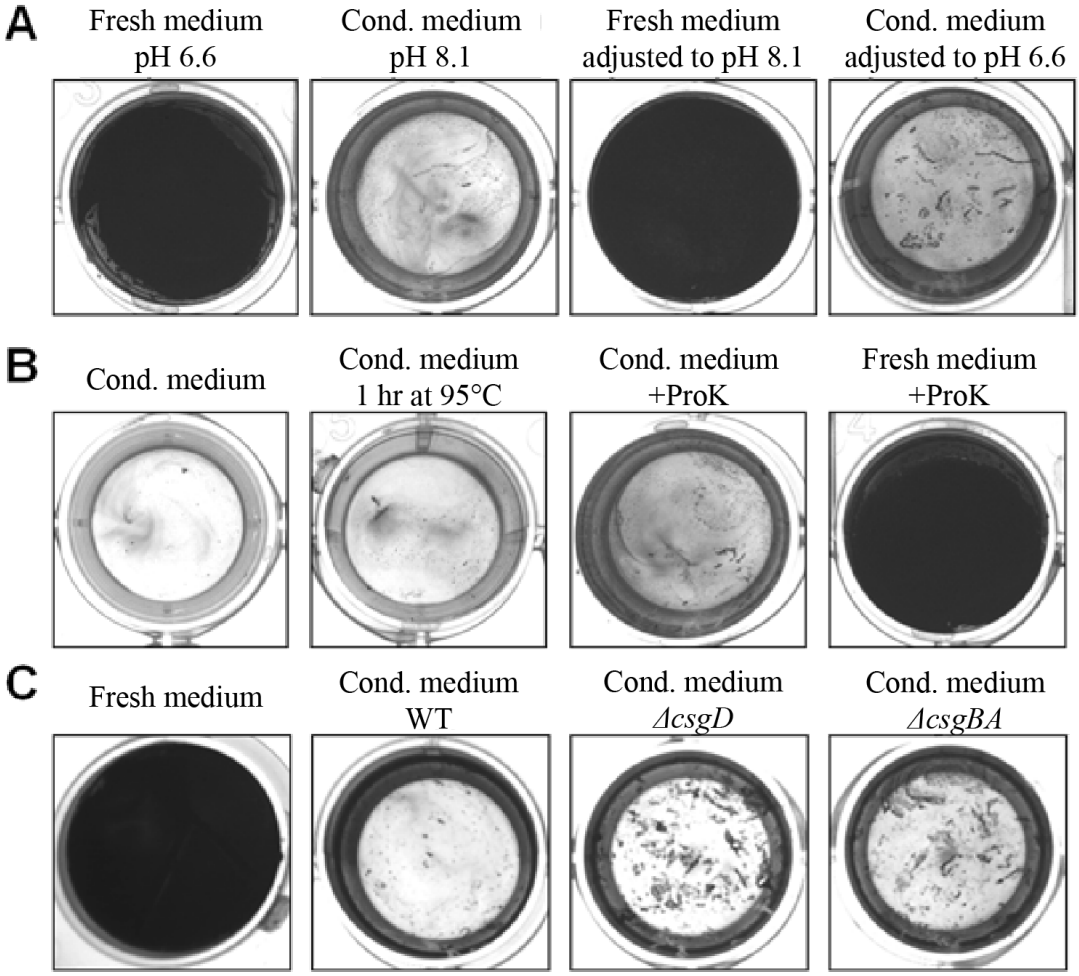

Figure 2.3: Molecular characterization of the conditioned medium. (A) Increase of pH in the conditioned medium was not responsible for the antibiofilm activity. UTI89 grown statically at 26°C for 48 hours in fresh medium (pH 6.6), conditioned medium (pH 8.1), fresh medium with pH adjusted to 8.1, and conditioned medium buffered to pH 6.6. **(B)** The potential inhibitor in the conditioned medium was heat stable and was resistant to proteinase K treatment. UTI89 was grown at 26°C for 48 hours in conditioned medium, conditioned medium boiled at 95°C for 1 hour, conditioned medium treated with 0.2µg/mL proteinase K, or fresh medium treated with proteinase K for 3 hours. Prior to inoculation, proteinase K in the medium was deactivated by boiling at 95°C for 1 hour. **(C)** Pellicle defective bacteria were able to produce the potential biofilm inhibitor. UTI89 was grown in fresh medium, or conditioned media collected from wild-type, Δ*csgD* or Δ*csgBA* at 26°C for 48 hours. Wells were stained with crystal violet.

cultures of Δ*cysE* or Δ*cysK*Δ*cysM* were supplemented with exogenous cysteine at various concentrations from 20µM to 200µM, grown for 4 days, and the resulting conditioned media was collected. Conditioned media from the Δ*cysE* or Δ*cysK*Δ*cysM* supplemented with cysteine regained the antibiofilm activity (Figure 2.3C). Remarkably, incubation of the Δ*cysE* or Δ*cysK*Δ*cysM* cultures with 20µM cysteine was sufficient to restore

the antibiofilm activity of the resulting conditioned media. Supplementation of Δ*cysE* or Δ*cysK*Δ*cysM* mutants with cystine also restored the antibiofilm activity of the conditioned media collected from these two mutants Figure 2.3D). Together, these results demonstrate that the antibiofilm activity of UTI89 conditioned media is dependent on cysteine/cystine metabolism.

Cysteine itself did not directly function as a biofilm inhibitor, as pellicle formation was not prevented in the fresh medium supplemented with cysteine (Figure 5.4A). Consistent with this results, post-addition of cysteine to conditioned media collected from a Δ*cysE* and Δ*cysK*Δ*cysM* cultures did not complement the antibiofilm effect (Figure 5.4B). Moreover, the precursor OAS also showed no inhibitory impact on pellicle formation in the fresh medium (Figure 5.4C).

Cysteine is a strong reducing agent involved in intracellular redox balance [99, 108]. Addition of the strong reducing agent dithiothreitol (DTT) did not affect pellicle formation (Figure 5.5A). Other thiols including glutathione (GSH) and D-cysteine also had no effect on pellicle formation in the fresh medium (Figure 5.5A). Conditioned media from glutathione mutants, Δ*gshA* and Δ*gshB*, still maintained antibiofilm activity similar to wild-type (Figure 5.5B). In addition, incubation of Δ*cysE* or Δ*cysK*Δ*cysM* mutants with DTT, glutathione, or D-cysteine did not restore the antibiofilm activity of the resulting conditioned cultures (Figure 5.5C and data not shown). Collectively, these results suggest the antibiofilm activity is related to cysteine/cystine and is not due to alteration of redox state.

2.3.3 Deficient biofilm formation in conditioned media coincided with reduced curli production

Pellicle development is dependent on curli production [22, 59]. We asked if curli expression in UTI89 grown in conditioned media was reduced. Curli production in UTI89 grown in fresh medium, diluted fresh medium, or conditioned medium collected from

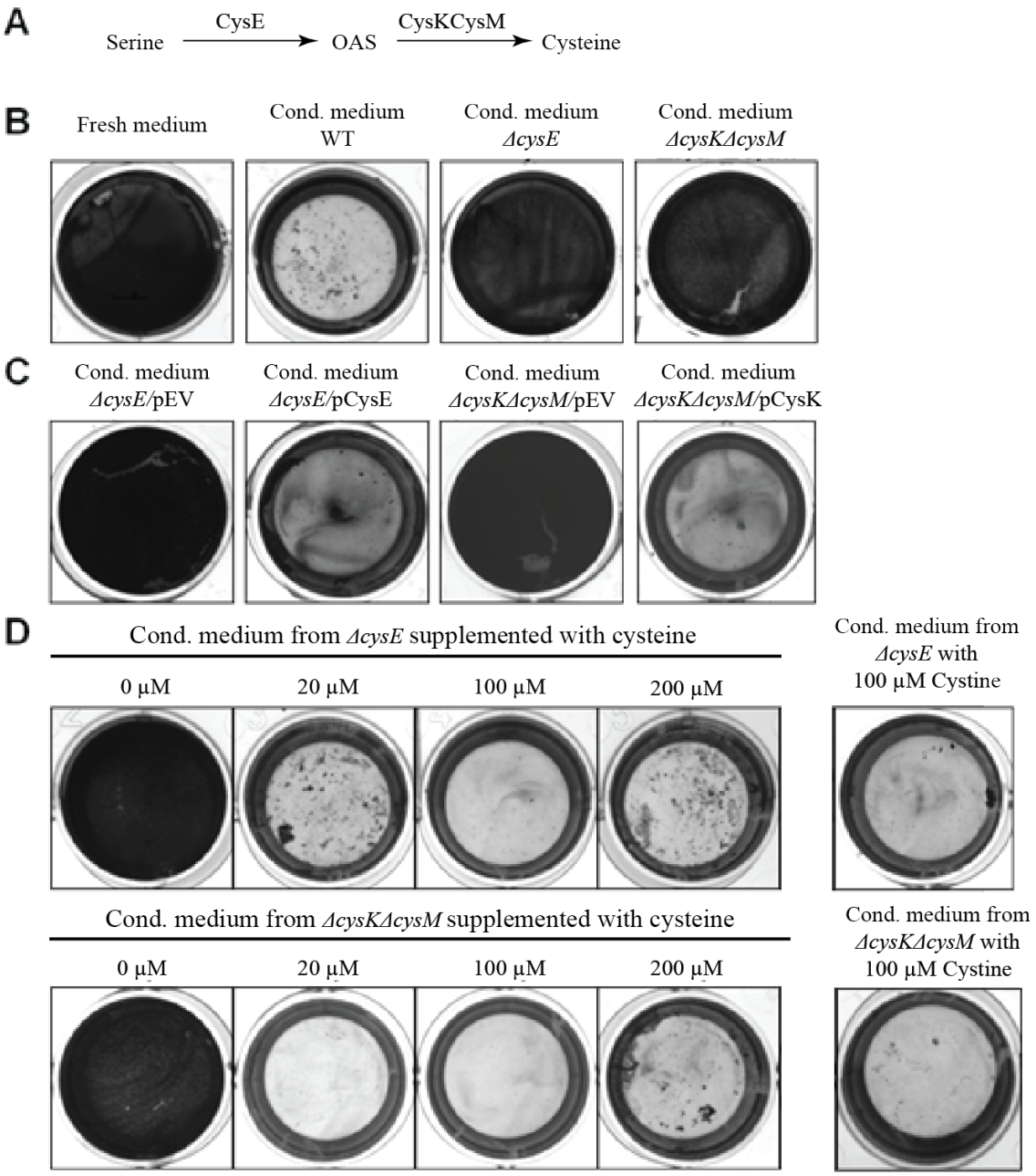

Figure 2.4: The biofilm-inhibitory effect of the conditioned medium was dependent on L-cysteine metabolism. (A) Schematic of cysteine biosynthesis mediated by the serine acetyltransferase CysE and OAS sulfhydrylases CysK and CysM. **(B)** Conditioned media collected from Δ*cysE* and Δ*cysK*Δ*cysM* lost biofilm inhibitory effect. **(C)** UTI89 grown at 26°C for 48 hours in fresh medium, or conditioned media collected from 4 day old cultures of wild-type, Δ*cysE*, Δ*cysK*Δ*cysM*, Δ*cysE*/pCysE, or Δ*cysK*Δ*cysM*/pCysK. **(D)** Supplementation of cysE and cysKcysM cultures with cysteine restored the antibiofilm activity of the conditioned medium. UTI89 wild-type, Δ*cysE* and Δ*cysK*Δ*cysM* were grown statically in YESCA medium supplemented with 20μM, 100μM, or 200μM, or 100μM cystine. After 4 days of growth at 26°C, corresponding conditioned media were collected and tested for the ability to support pellicle formation of UTI89 wild-type at 26°C for 48 hours. Wells were stained with crystal violet.

4 day old wild-type UTI89 culture was analyzed by western blot (Figure 2.4A). UTI89 grown in the fresh medium or the diluted fresh medium for 24 hours produced bacteria associated CsgA, whereas no CsgA was detected from UTI89 grown in the wild-type conditioned medium (Figure 2.4A). Interestingly, curli production was partially restored in UTI89 grown in conditioned media collected from a Δ*cysE* culture and a Δ*cysK*Δ*cysM* culture (Figure 2.4A).

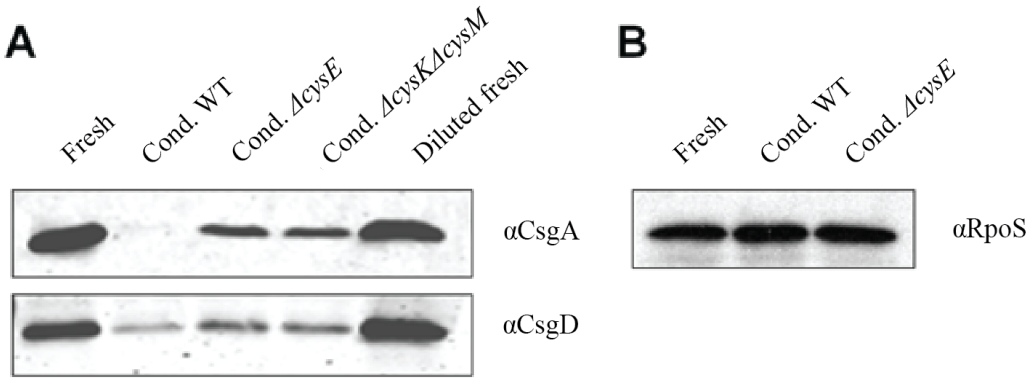

Figure 2.5: Curli production was reduced in UTI89 grown in the conditioned medium. (A) UTI89 was grown at 26°C in fresh YESCA, diluted fresh YESCA, or conditioned media collected from cultures of wild-type, Δ*cysE* mutant or Δ*cysK*Δ*cysM*. After 24 hours of growth when the biofilm had just started to form, all bacteria in the well, including the pellicle and planktonic cells, were collected for Western blot analysis. To detect curli production, cell lysates were pre-treated with HFIP. Cell lysates without HFIP treatment were used for the CsgD blot. The blots were probed with *α*CsgA or *α*CsgD antibody, respectively. **(B)** UTI89 was grown at 26°C for 24 hours in fresh YESCA, diluted fresh YESCA, or conditioned medium collected from wild-type UTI89 culture. Bacteria from the pellicle and the planktonic bacteria were collected for Western blot. The blot was probed by *α*RpoS antibody.

2.3.4 Cysteine metabolism controls multiple biofilm models

In preparation of Δ*cysE* and Δ*cysK*Δ*cysM* cultures to produce conditioned media, we noticed that these cultures produced a pellicle at the air liquid interface, but the pellicle formed was smooth rather than the wrinkled pellicle that is normally seen in WT UTI89 (Figure 2.5 and Cegelski 2009). Supplementation of low levels of Congo red to YESCA media (1:7,500) allows for clear visualization of the topography present in the pellicles formed by UTI89 (Figure 2.5). Under similar growing conditions at low temperatures on YESCA agar, UTI89 develops rugose colony biofilms with distinctive wrinkles, sometimes

referred to as rdar (red, dry, and rough) [22,36] (Cegelski 2009, Depas 2013). The development of rugose biofilms is also dependent on curli and cellulose production. Thus, rugose biofilms appear to mirror the formation of wrinkles in pellicles. We hypothesized that if cysteine metabolism is important for the formation of wrinkles on pellicles, it may also be important for rugose colony wrinkle formation.

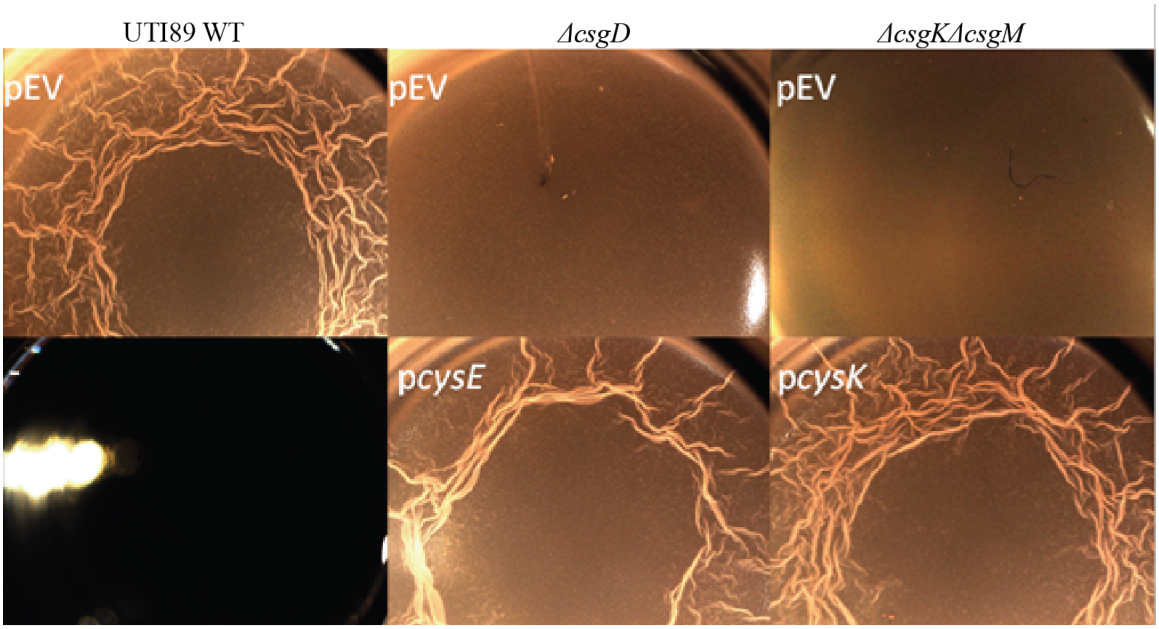

Figure 2.6: Cysteine auxotrophy inhibits pellicle wrinkling. Pellicles are inoculated via 2μL of overnight culture into 2mLs of fresh media. Pellicles were grown for 48 hours at 26°C in YESCA media supplemented with 1:7,500 YESCA:Congo red stock and 25μM IPTG. Cysteine auxotrophs formed smooth pellicles, while *in trans* complementation restored pellicle wrinkling. The negative well is a non-inoculated well of the pellicle media.

We determined that cysteine auxotrophy interrupted rugose colony spreading and wrinkling (Figure 2.6). Wrinkling of Δ*cysE* colonies can be restored by growing bacteria next to a sterile filter disk with 10% (m/v) cysteine or OAS. Δ*cysK*Δ*cysM* mutants had colony wrinkling restored by exogenous addition of cysteine but not by OAS addition (Figure 6A). The colony wrinkling was also restored by *in trans* complementation of either of these mutants (Figure 2.6B). The number of cells within the colony does not seem to affect colony wrinkling, ad addition of 250μM cysteine to YESCA media led to colony wrinkling in Δ*cysE* without statistically changing CRUs present within the colony (Figure 2.6C).

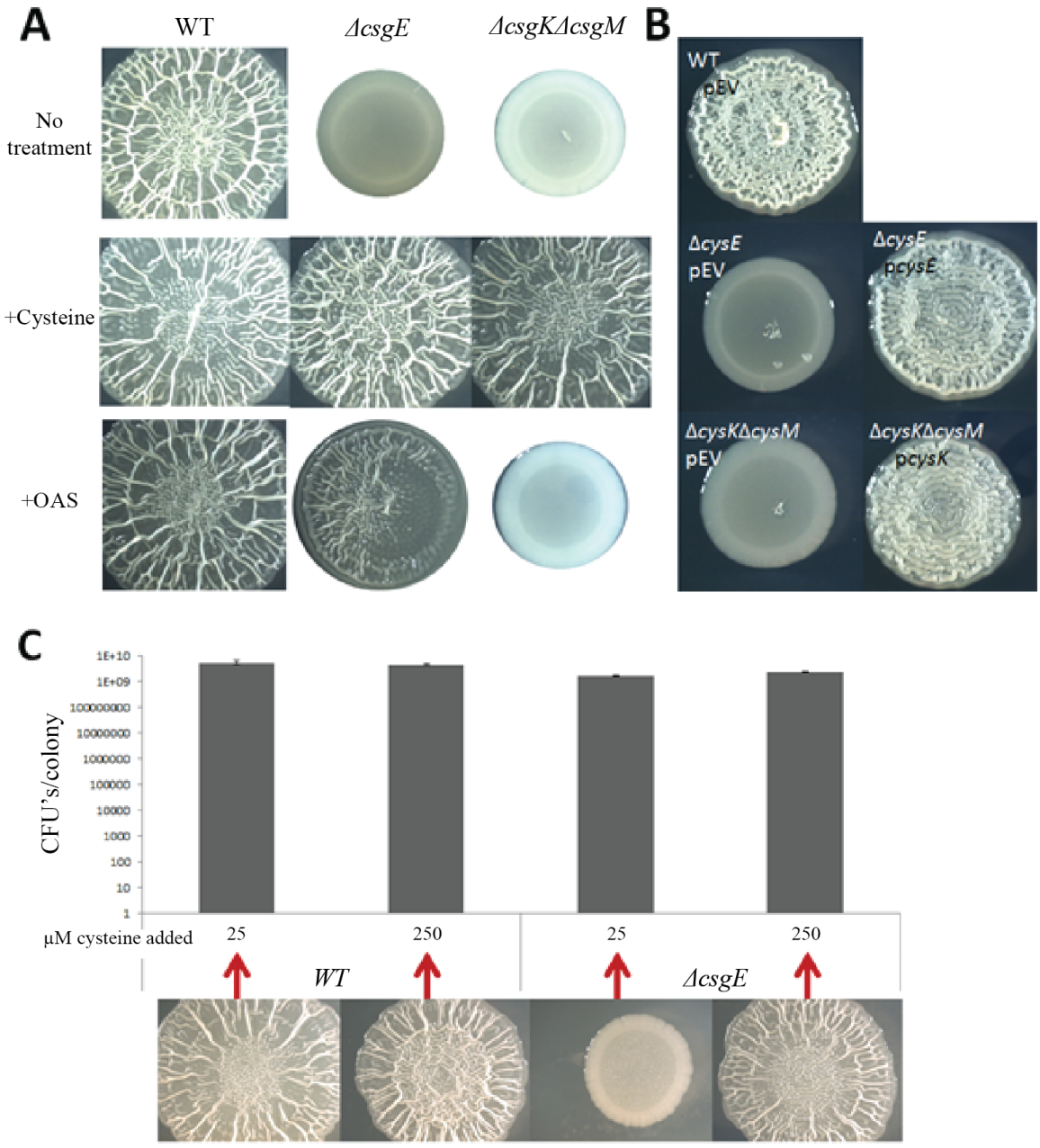

Figure 2.7: Cysteine auxotrophy inhibits rugose colony spreading and wrinkling. (A) Rugose colony biofilms grown at 26°C on YESCA media normally spread and wrinkle. Cysteine auxotrophy via Δ*cysE* or Δ*cysK*Δ*cysM* inhibits the wrinkling and spreading of rugose colonies. Exogenous supplementation of 10% (m/v) cysteine on a paper disk restores wrinkling to both cysteine auxotrophs. Exogenous supplementation with 10% OAS restores wrinkling to Δ*cysE* but not to Δ*cysK*Δ*cysM* as it can no longer convert this compound to cysteine. **(B)** *in trans* complementation of cysteine auxotrophs restores colony wrinkling. **C** WT and textitΔcysE rugose colonies grown on YESCA and YESCA supplemented with 25μM or 250μM of cysteine for 48 hours. Colonies were resuspended in 1mL of buffer and tissue homogenized prior to serial dilution and CFU determination.

The diguanylate cyclase AdrA was downregulated at the transcriptional level in the Δ*cysE* and Δ*cysK*Δ*cysM* colonies (Figure 2.7A). Supplementation of the cysteine auxotrophs with 250μM cysteine restored colony wrinkling and increased *adrA* transcription (Figure 2.7B). Rugose formation of Δ*cysE* was complemented by driving expression of *adrA* via the *csgBAC* promoter (pLR2)(Figure 2.7B), suggesting cystiene metabolism regulates rugose formation by modulating cellulose synthesis. Taken together, cysteine metabolism appears to play an integral role in the formation of pellicles and rugose biofilms.

2.4 Discussion

Many bacteria are capable of producing extracellular signals such as autoinducing peptides, D-amino acids, and indole to trigger biofilm disassembly or to prevent biofilm formation [81, 86, 116, 140, 146]. We found that UTI89 released an antibiofilm factor into the environment as the cultures aged (Figure 1).

Several molecules with antibiofilm activity have been discovered in *E. coli* cultures that display antibiofilm activity [86,146]. It reduces biofilm formation of *E. coli* K12 strains through the homoserine lactone transcriptional regulator, SidA [86, 87]. Although indole and indole derivatives have been reported to efficiently decrease biofilm formation of various *E. coli* strains [86], they do not seem to affect pellicle formation of UTI89, as robust pellicles were formed in the presence of millimolar concentrations of indole (Figure A2A). Moreover, the fact that the indole synthase mutant Δ*tnaA* was still able to produce antibiofilm activity suggests indole or its derivatives are not pellicle inhibitors (Figure A2A). Additionally, a Δ*sdiA* mutant was unable to form a pellicle in the conditioned medium (data not shown). Uropathogenic *E. coli* also produces and releases soluble capsular polysaccharides that prevent surface attachment and biofilm formation of a broad spectrum of gram-negative and gram-positive bacteria [140]. However, group II capsular polysaccharide was not responsible for the antibiofilm activity against pellicles as conditioned media from capsular polysaccharide synthesis mutants Δ*kpsF* and Δ*kpsS* did not

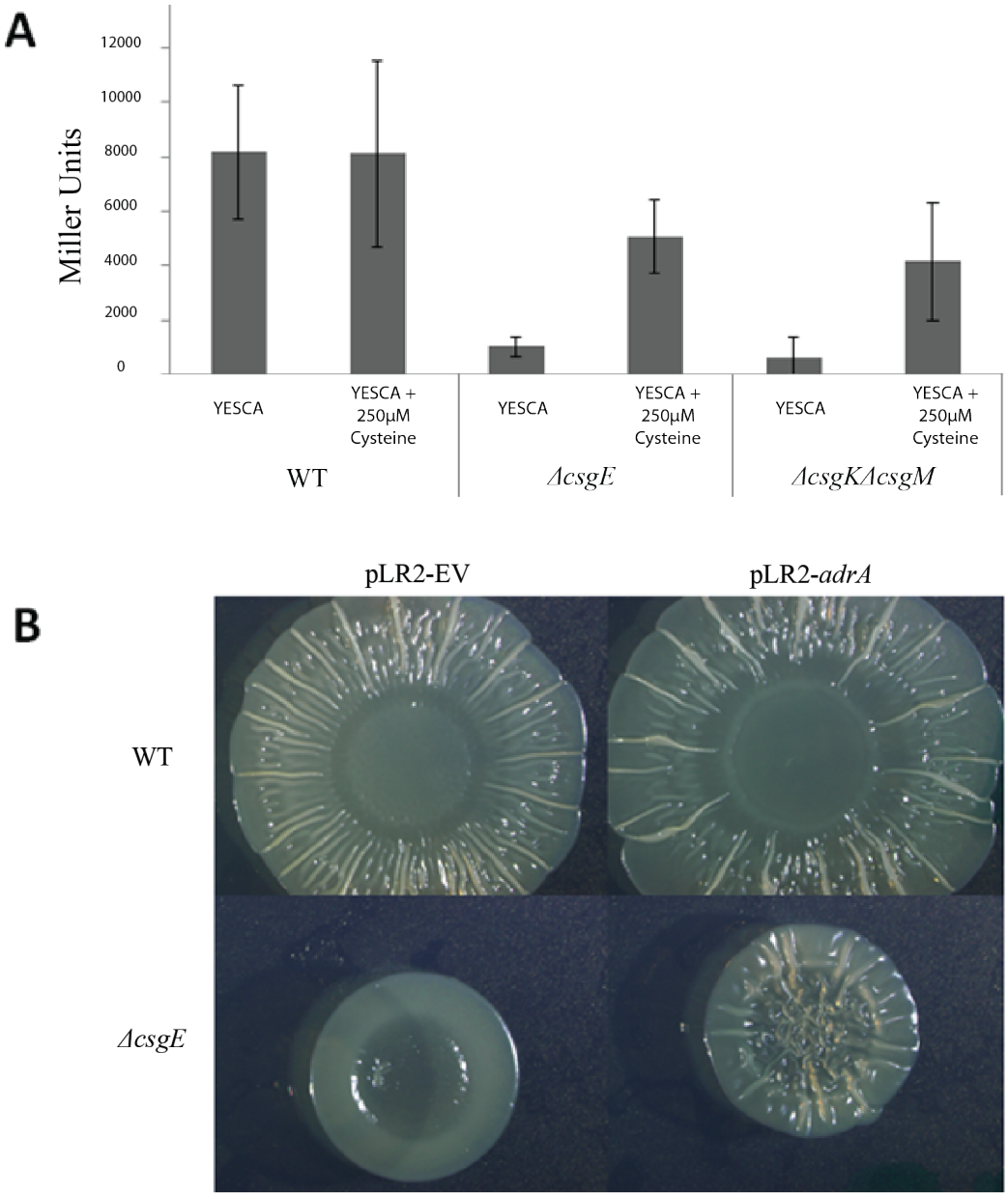

Figure 2.8: Decreased *adrA* transcription causes smooth colonies in cysteine auxotrophs. (A) Miller assays with the *adrA* promoter upstream of *lacZ*. Colonies were grown for 48 hours at 26°C on YESCA media or YESCA media supplemented with 250μM cysteine. Miller assays were performed in biological triplicate on all samples. **(B)** The *csgBAC* promoter driving *adrA* expression (plr2-*adrA*) restores wrinkling in Δ*cysE* colonies grown for 48 hours at 26°C.

inhibit pellicle formation (Figure A2B). Additionally, we analyzed norspermidine and D-amino acids since both of them showed antibiofilm activity and were released in aged pellicle biofilm culture of *B. subtilis*. However, neither D-amino acids, norspermidine, nor the combination of the two agents had any inhibitory affect on UTI89 pellicle development

under the conditions tested (Figure S2C).

We found that the antibiofilm factor that is present in UTI89 conditioned media is dependent on cysteine biosynethesis genes (Figure 3). High concentrations of sulfhydryl compounds including cysteine were reported to inhibit biofilm formation in *S. aureus* by reducing biosynthesis of polysaccharide intracellular adhesin [156]. *E. coli* exports cysteine and its precursor OAS [31, 50, 99], and genes involved in cystiene biosynthesis play a role in modulating biofilm development [38, 128]. Sturgill *et al.* showed that an *E. coli* MG1655 Δ*cysE* mutant, which is unable to catalyze the conversion of serine to OAS, exhibits accelerated biofilm formation with increased biomass, suggeting that cysteine or OAS may act as a biofilm inhibitor intracellularly or extracellularly [131]. We have demonstrated that conditioned media from niether Δ*cysE* nor Δ*cysK*Δ*cysM* were able to inhibit pellicle biofilm development, and the antibiofilm activity can be restored efficiently by supplementing the mutant cultures with cysteine or cystine (Figure 3), suggesting that the antibiofilm factor in the wild-type conditioned medium is dependent on cysteine/cystine metabolism and is downstream of OAS. The antibiofilm activity seems to be specially mediated by cysteine/cystine, as other thiols including GSH, D-cystine, and DTT were unable to restore the antibiofilm activity (Figure S5). It is unclear how cysteine/cystine metabolites serve to prevent pellicle development. Cystiene or the precursor OAS did not impair pellicle development when added directly to fresh cultures even at millimolar concentrations (Figure S4). Consistent with this result, we did not detect a significant difference of extracellular cysteine concentration between the fresh medium and the conditioned medium quantified by the method of Gaitonde (49)(data not shown). Aditionally, the inhibitory effect is not likely a result of altered redoc balance, as addition of other reducing agents such as DTT and glutathione to Δ*cysE* or Δ*cysK*Δ*cysM* cultures did not restore biofilm inhibition (Figure S5).

Cysteine metabolism also controls pellicle and rugose biofilm formation. In paying close attention to our Δ*cysE* and Δ*cysK*Δ*cysM* cultures destined for conditioned media

production, we noticed the cysteine auxotrophs form smooth pellicles. These smooth pellicles can be complemented *in trans* to develop pellicle wrinkles that look like the WT wrinkles (Figure 2.5). This smooth morphotype is mirrored in rugose biofilm formation, as cysteine auxotrophs form smooth unwrinkled colonies in this biofilm type. These biofilms can be complemented exogenously by cysteine, and Δ*cysE* can also be complemented by OAS. Δ*cysE* still can produce both OAS sulfhydrylases, CysK and CysM, which can convert OAS to cysteine, but Δ*cysK*Δ*cysM* still has a smooth colony with exogenous OAS addition, as it cannot further convert OAS to cysteine. This provides support that this biofilm modulation signal is downstream of OAS and is dependent on cysteine metabolism. It also means that the wrinkled phenotype is not a CysB mediated transcriptional change. CysB is a LysR type regulator that has DNA binding activity in the presence of N-acetylserine (NAS), which is produced from OAS at high pH8? or higher. If the wrinkling was mediated by CysB colonies of ΔcysKΔcysM would wrinkle when exposed to OAS at pH?, as OAS could still be converted to NAS, thus activating CysB. We previously observed the oxidative stress plays a role in rugose biofilm formation. However, addition of oxidant or reducing agent (DTT) to cysE mutant did not rescue rugose biofilm formation.

There are several possible mechanisms of how cysteine mediates the production antibiofilm activity in conditioned cultures. One possibility is that a cysteine breakdown product or multiple products may have additive inhibitory effects. To keep intracellular cystiene in balance, bacteria degrade cysteine into hydrogen sulfide, ammonia and pyruvate [9, 10, 35, 93, 95]. Although none of these compounds were found to inhibit pellicle formation (Figure A5 and data not shown), we cannot rule out the possibility that an accumulation of these metabolites have additive effects against biofilm formation. Alternatively, cysteine metabolism in aged cultures may lead to alteration of other metabolic pathways. Cysteine is linked to homocysteine and methoionine biosynthesis and other sulfur metabolism [122]. An imbalance of intracellular cysteine may also affect the metabolic network. Biofilm development is sensitive to subtle changes in environmental cues includ-

ing nutrient composition, levels of phosphate, and osmolarity [79]. Thus, subtle changes in extracellular amino acids level or sulfur metaboites may result in deficient pellicle formation. Additionally, in cysteine-methionine pathway, methionine can be converted to S-adenosyl-methionine (SAM), which is related to quorum sensing molecules such as AI-2. Therefore, manipulation of cysteine biosynthesis may affect the production of a potential downstream signaling molecule.

2.5 Acknowledgements

Yizhou Zhou spearheaded this project and helped with the experimental designs. Alexandra Christensen, an undergraduate student working with me in the laboratory, helped in testing various auxotrophs.

CHAPTER III

Real-time fluorescence microscopy assay for amyloid aggregation

3.1 Introduction

Parkinson's disease is a neurodegenerative disease that is characterized by intra-synaptic deposits found in Lewy bodies and Lewy neurites in the brains. The major components of these deposits are α-synuclein amyloid fibers [121, 143, 153]. α-synuclein is a short, intrinsically disordered protein that can be found at relatively high concentrations, up to 50μM, at neuronal synapses [152].

The aggregation of α-synuclein to form fibrous amyloid structures is also associated with a variety of other neurological disorders, including Alzheimer's disease and Huntington's disease [27,34,55,130], though neither the molecular mechanisms by which these proteins form these aggregates nor the source of their toxicity is yet understood [34].

Recently, studies have shed light on the role that intestinal microbes play in overall health [145]. Much interest has focused on the role that these microbes play in brain function [51]. Enteric bacteria such as *Escherichia coli* secrete extracellular amyloid fibers called curli which share many of the same structural and biophysical properties as disease associated amyloids [23]. Unlike disease associated amyloids, curli fibril formation is highly regulated by a dedicated assembly pathway [23, 30, 72, 127]. Curli are responsi-

ble for facilitating adhesion to surfaces, invasion of host cells, biofilm development, and pathogen-host interactions, as well as regulating inflammatory and immune responses in the gut [8, 13, 85, 104, 137, 138, 144]. Curli have been shown to trigger α-synuclein aggregation through a process known as cross-seeding [24]. In vitro, amyloids polymerize into fibers with nucleation dependent kinetics in three distinct phases; the lag phase, the growth phase, and the stationary phase [7, 123]. In the lag phase, monomers assemble into on-pathway oligomeric nuclei . Once these oligomeric intermediates are formed, they catalyze fiber elongation in the growth phase (Figure 3.1). Formation of these oligomers is the rate-limited step and can take considerable time. However, add a preformed fibrils to the solution – seeding – decreases or eliminates this lag phase [7, 123]. Cross-seeding is when an amyloid of one type causes an amyloid of another to adopt the same structure and it has been well documented [90, 159]. However, it is not yet well understood are how fibril formation is initiated nor how fibrils can template further fibril polymerization.

One way to address these questions is to measure the rates at which interactions between molecules occur. However, quantitatively measuring the kinetics of protein aggregation is quite a challenging problem, and many powerful techniques are often unavailable for the study of amyloids because of their insolubility. The most commonly carried out measurements are made in bulk assays in which an ensemble of protein aggregates at various stages of fibril formation is monitored. These methods can further be broken down into two categories: *in situ*, during the reaction, and *ex situ*, that require that aliquots are taken from the reaction at defined time-points [7]. Many of these techniques yield different information about the sample and each technique has advantages and disadvantages depending on the aim. Therefore, many are often used together to paint a more complete understanding of the reaction. However, these types of experiments mask the complexity of macromolecular interactions which are by nature, stochastic at the molecular level. Descriptions of fibril growth by a single rate constant captures the average behavior. Furthermore, such fundamental questions such as for this reason, it's useful to try to follow

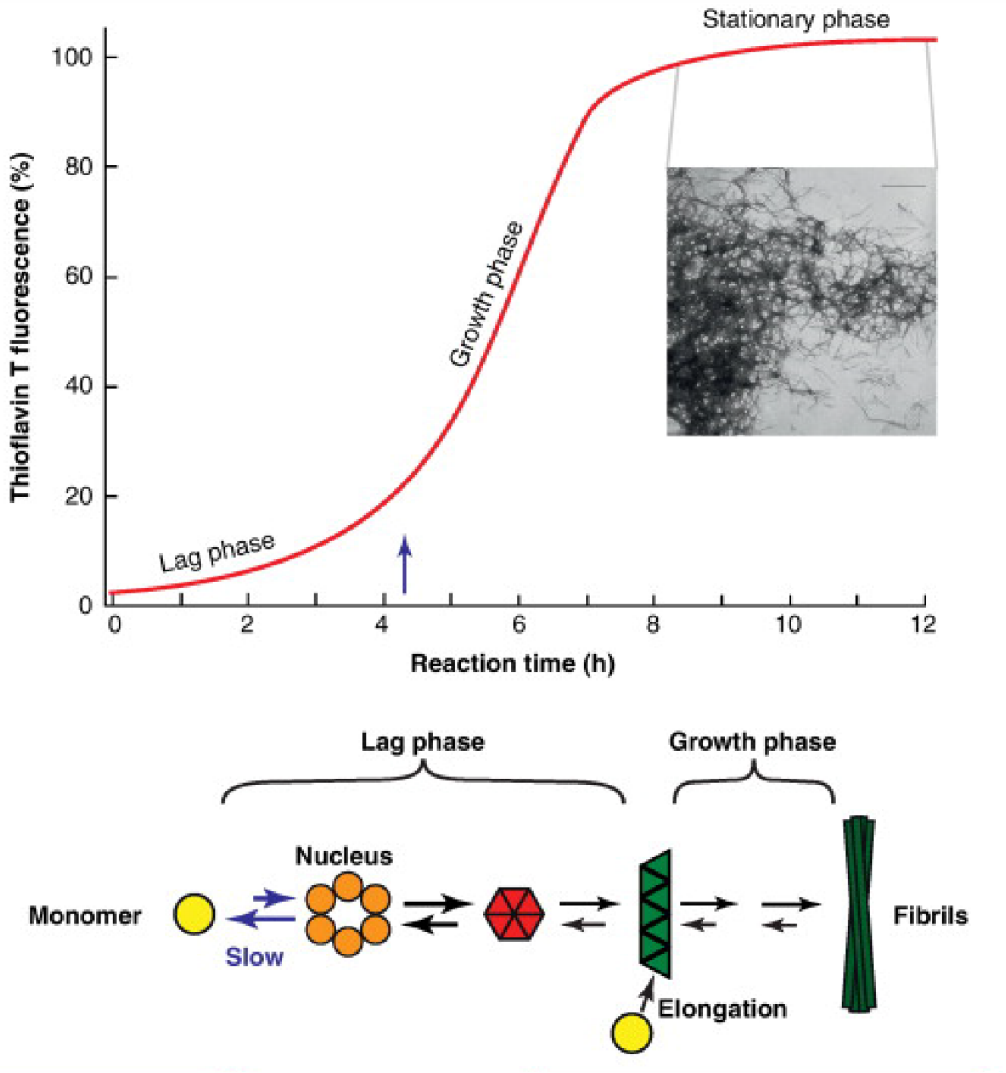

Figure 3.1: Kinetics of *in vitro* amyloid polymerization as monitored by ThT. This schematic illustrates protein monomers polymerizing into amyloid. The lag phase, growth phase, and stationary phases are indicated. The blue arrow indicates the end of the lag phase. Figure reproduced from reference [17]

the reaction at the level of single molecule.

The early stages of aggregation have been studied using single molecule fluorescence techniques. The diffusion of fluorescently labeled protein molecules was measured through the focal volume of a laser [105]. And the growth of individual fibers have been monitored by such methods as total internal reflection fluorescence microscopy (TIRF) and dSTORM (direct stochastic optical reconstruction microscopy) [12,109]. TIRF has enabled views into the nature of fibril formation and revealed such features as polarized fiber

growth and stop-and-go kinetics [2, 45, 154, 157]. For these reasons, we aimed to extend the TIRF method in combination with bulk ensemble methods to characterize CsgA and α-synuclein cross-seeded fibril formation.

3.2 Experimental procedures

3.2.1 CsgA purification

CsgA was purified as previously described [44]. Briefly, expression of C-terminal His_6-tagged CsgA or CsgB homologs without the Sec signal sequence in NEB3016 was induced at $OD_{600} = 0.9$ by 0.5 mM IPTG at 37°C for 1 hour. Bacteria were lysed in 8 M guanidine hydrochloride in 50 mM potassium phosphate buffer (KPi) overnight at 4°C. After centrifugation at 10,000 x g for 20 minutes, the supernatant was incubated with nickel-nitrilotriacetic acid (Ni-NTA) resin (Sigma Aldrich) at room temperature for 1 hour and then loaded onto a disposable polypropylene column (Thermo-Fisher). Proteins were eluted into 50 mM KPi containing 125 mM imidazole. To get monomeric CsgA, fractions with the target protein were combined and loaded onto a 30-kDa centrifugal filter units (Thermo-Fisher) to remove dimers and other oligomers. To make CsgA seeds, 2 week-old fibers were sonicated for three 10 second bursts on ice.

3.2.2 α-synuclein purification

The protein purified using the protocol described previously with minor modifications [142]. Briefly, 1% of the overnight grown culture was transferred in fresh media and induced with 0.8 mM IPTG (Isopropyl β-D-1-thiogalactopyranoside) for four hours after the optical density (O.D.) of the culture reached to 0.6. The induced cells were pelleted at 4,000 rpm and resuspended in 25 mL lysis buffer (10 mM Tris, 1 mM EDTA, pH 8). The lysed cells were then boiled at 95°C for 15-20 minutes and centrifuged at 11,000 rpm for 20 minutes. The supernatant was thoroughly mixed with 10% streptomycin sulfate

solution (136 μL/ml) and glacial acetic acid (228 μL/ml). The solution was centrifuged at 11,000 rpm for 30 minutes. To the clear supernatant, equal volume of saturated ammonium sulphate was added and incubated at 4°C for an hour with an intermittent mixing. The precipitated protein was separated by centrifuging it at 11,000 rpm for 30 minutes. The pellet was dissolved in equal volume of absolute ethanol (chilled) and 100 mM ammonium acetate. Finally, the pellet was washed with absolute ethanol, dried at room temperature and resuspended in 50 mM Tris pH 7.2. The protein solution was filtered through 50 kDa cutoff column (Amicon, Millipore). The protein was checked on SDS-PAGE and the molecular weight was confirmed by Mass Spectrometry. The concentration of protein was determined using $\epsilon_{275} = 5,600 M^{-1} cm^{-1}$. The purified proteins were stored at -80°C at concentration of 100 μM until use.

3.2.3 Thioflavin T assay

Freshly purified CsgA was diluted in 50mM KPi (pH 7.3) to the molar concentration indicated in each experiment. Samples were incubated along with 20 μM ThT in a black, flat-bottom 96-well plates (Corning) which were sealed with a transparent microplate sealer. Plates were incubated at 25°C. Readings of the ThT fluorescence intensity were taken at 15 minute intervals following a 5 seconds orbital mixing for 24 hours.

α-synuclein was thawed on ice, syringe filtered, and diluted in 50mM KPi (pH 7.3) to the molar concentrations indicated in each experiment. 20 μM ThT was incubated with 75 μL of 50 μM α-synuclein with 20μM ThT and 100mM NaCl and a 2mm glass bead for homogeneous mixing. Plates were incubated under continuous orbital shaking conditions on a Tecan plate reader at 300 rpm at 37°C. Readings of ThT fluorescence intensity at 495 nm were collected every 30 minutes or hour for 48-72 cycles in the top excitation/emission mode.

In cross-seeding experiments, freshly purified CsgA and α-synuclein were diluted in 50 mM KPi, (pH 7.3) to the molar concentrations indicated in each experiment. Samples

were incubated in 96-well, black, flat bottom plates at 37°C with 20μM ThT and 100 mM NaCl under continuous shaking conditions, along with a 2mm glass bead for homogeneous mixing. The ThT fluorescence intensity was recorded in 30 minute intervals using a Tecan plate reader (excitation: 438 nm; emission: 495 nm; cut-off: 475 nm).

3.2.4 Transmission electron microscopy

5μL of the sample was applied to formar coated carbon-coated grids (Ernest F. Fullam, Inc, Latham, NY) and incubated for 1 minute, washed with MilliQ water before negatively staining with 1% uranyl acetate for 90 seconds. Samples were imaged on Jeol electron microscope (JEOL1400 plus).

3.2.5 Protein labeling

The proteins were expressed and purified as described above. Proteins were labeled as previously described [109]. Briefly, α-synuclein was labeled at the C-terminus at residue 122. This residue lies outside the proposed amyloid forming region of the protein. ThT fluorescence measurements were performed to ensure that the mutation did not interfere with aggregation kinetics (data not shown). CsgA was labeled at the 150 position, also located at the C-terminus of the sequence. This mutant has previously been shown to behave like wild-type *in vivo* and assembles *in vitro* similarly to wild-type.

The CsgA Q150C and α-synuclein N122C were labeled with maleimide-modified Alexa Fluor 647 dye (Invitrogen, Carlsbad) via a cysteine thiol moiety. Labeled protein was purified from the excess free dye by a P10 desalting column via Sephadex G25 matrix (GE Lifesciences).

3.2.6 TIRF microscopy

Imaging was performed on flow cells and 16-well culture wells (Grace BioLabs). Wells were passivated by overnight incubation in 5% (w/v) Pluronic acid (Thermo-Fischer), and

washed thoroughly. Imaging was done using a Nikon Ti2-E motorized inverted microscope with LED-based light sources (100x, 1.45NA) with a Photometrics Prime 95B Back-illuminated sCMOS Camera. Image analysis was performed using Fiji v 1.0.

3.3 Results

3.3.1 ThT establishes that mutants can cross-seed

The kinetics of polymerization for both CsgA and α-synuclein have been widely studied and are known to exhibit three characteristic states: the lag phase, the growth phase, and the stationary phase [43]. First, it was necessary to confirm that in the Chapman lab conditions CsgA was able to accelerate α-synuclein aggregation. Fibril formation was monitored by ThT fluorescence. The addition of freshly purified, monomeric CsgA to α-synuclein decreased the rate of α-synuclein aggregate formation. Additionally, the slope of the sigmoidal curve became steeper indicating a more cooperative transition than α-synuclein alone (Figure 3.2).

Interestingly, the addition of pre-formed CsgA fibrils only modestly affected α-synuclein amyloid formation (Figure 3.4). Pre-formed CsgA seeds did not catalyze the aggregation process of α-synuclein as well as soluble CsgA, but the effect was concentration dependent. This concentration dependence of the acceleration of α-synuclein could be attributed to the increasing concentration of monomer in solution as the seed concentration was increased. It was hypothesized that these monomer species were responsible for interacting with α-synuclein and precipitated the resultant increase in kinetics (Figure 3.2 and 3.3). Lending support to this hypothesis is the fact that others in the lab have been unable to detect interactions between CsgA and α-synuclein in surface plasmon resonance experiments (unpublished data). This suggested that the interactions between the two proteins is quite transient.

To test the effect of α-synuclein on CsgA fibril formation, a similar experiment was

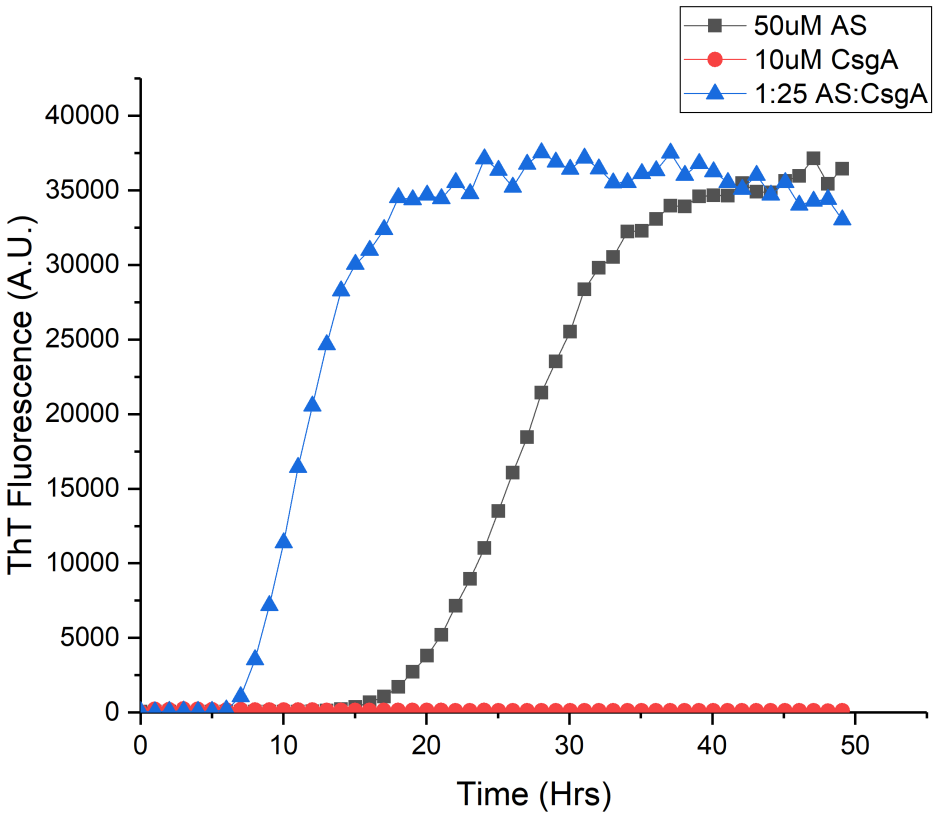

Figure 3.2: Addition of CsgA accelerated the polymerization of α-synuclein.In black, ThT fluorescence of of monomeric α-synuclein. In red, ThT fluorescence of monomeric α-synuclein incubated at a 25:1 molar ratio with freshly purified CsgA.

carried out. Soluble α-synuclein and α-synuclein seeds were added to soluble CsgA and fibril formation was monoitored by ThT fluorescence. Results showed that soluble α-synuclein decreased the rate of aggregation in CsgA (Figure 3.5) but preformed α-synuclein seeds had no effect on CsgA aggregation (Figure 3.6).

3.3.2 Single-molecule tracking of amyloid formation

In order to carry out the TIRF experiments with labeled protein, a series of CsgA and α-synuclein mutants were constructed with cysteine residues inserted at various locations that can be labeled with maleimide cysteine thiol reactive flourescent dyes. Neither CsgA nor α-synuclein contain a cysteine in their primary sequence. The thiol groups are particularly powerful in this instance as the engineered sites allowed precise and selec-

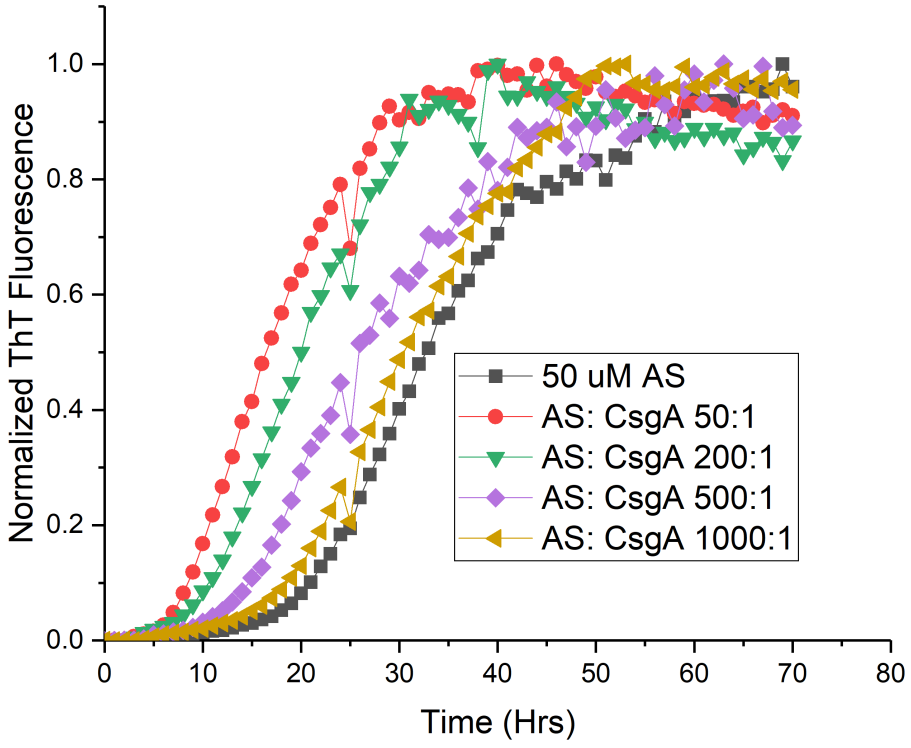

Figure 3.3: Monomeric CsgA accelerated the polymerization of α-synuclein in a concentration dependent manner. ThT fluorescence of 50μM α-synuclein with CsgA monomer at various molar ratios shows that increasing concentration of CsgA increasesd the rate of α-synuclein polymerization.

tive labeling. The maleimide group reacts at with the thiols at neutral pH to form a stable linkage that is not reversible and does not react with tyrosines, histidines, or methionines [68]. Direct covalent linkage of the dye to the protein was an appealing method as compared to techniques such as immunofluorescence staining because of the the small size of the dye molecules compared to antibodies [78, 113]. These factors all contributed to an increase in resolution of the imaging process.

To ensure that *in vitro*, the mutants assembled into amyloid fibers efficiently when compared to wild-type as measured by ThT, a CsgA Q150C mutant that had previously been tested in the lab *in vivo* and had been found to be wild-type like was chosen [147]. ThT assays further illustrated that it behaved closely to wild-type in kinetic experiments

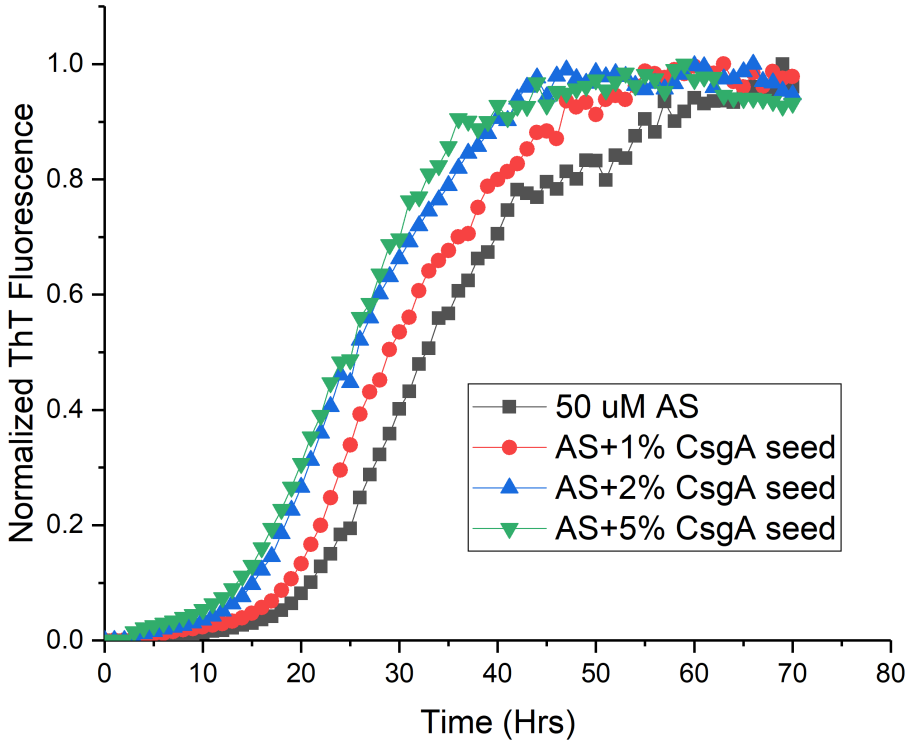

Figure 3.4: CsgA seeds did not accelerate the polymerization of α-synuclein as much as soluable monomeric CsgA. ThT fluorescence of 50μM α-synuclein with CsgA at increasing concentration of seeds showed a slight concentration dependence which likely results from an increase in monomer concentration.

with batch to batch variability in is taken into account (Figure 3.7).

In reading the literature, several promising potential α-synuclein mutants for these assays were identified. Previous work on a N122C mutant seemed most promising. The mutation is located at the N-terminus and well outside the NAC region of the protein which is thought to be responsible for aggregation [109]. ThT polymerization data showed that the mutant and WT α-synuclein showed similar aggregation kinetics so so it was chosen for the following experiments (Figure 3.7).

For both proteins in the absence of the AlexaFluor label, because of the cysteine mutation, a small concentration of reducing agent was required to ensure that disulfide bonds did not form. The effect of the reducing agent on the kinetics of fibril formation on wild-

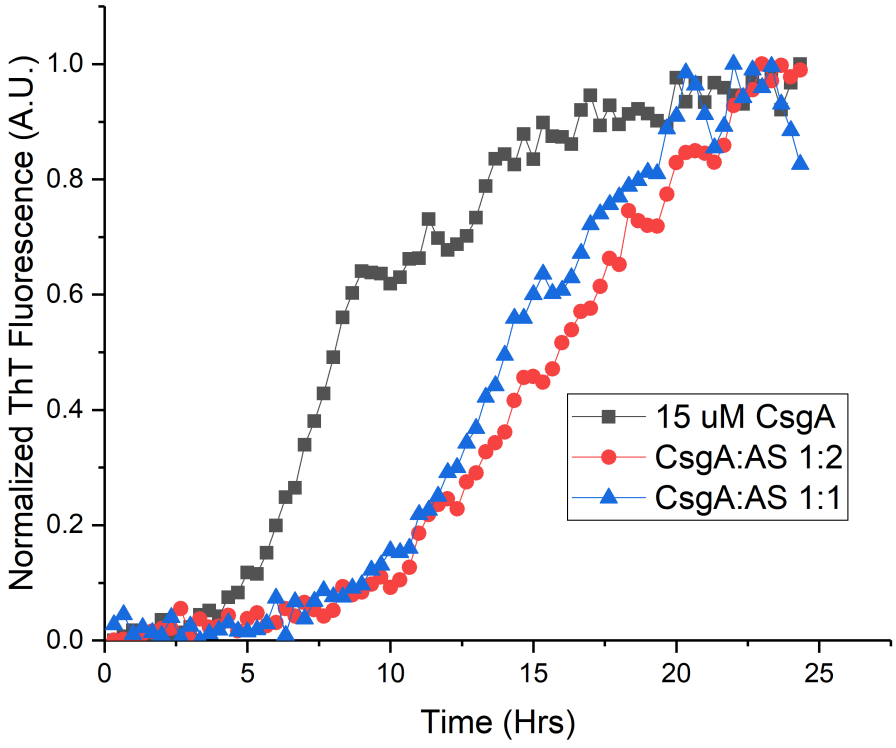

Figure 3.5: Soluble α-synuclein decreased the rate of CsgA fibril formation. Monomeric α-synuclein at molar ratios of 1:1 and 1:2 decreased the rate of CsgA fibril formation.

type protein was also tested (data not shown).

Next, the effect of adding the AlexaFluor dye to the protein was tested in ThT experiments. Unsurprisingly, high ratios of dye to protein were found to affect kinetics (Figure 3.9). But decreasing the concentrations of dye to protein and by playing with the ratios of labeled to unlabeled protein, the effect of the fluorophore on the structure of the fibril and effects on the kinetics was minimized (Figure 3.10A). Interestingly, TEM images of the resulting fibers do not show major differences in morphology between the mutants and wild-type fibrils (data not shown).

To establish that it is possible to visualize both proteins using this technique, varying ratios of labeled to unlabeled protein were incubated in 16 well culture wells. The aim was to find a ratio that would give good resolution. Visualization of the growth of CsgA fibrils

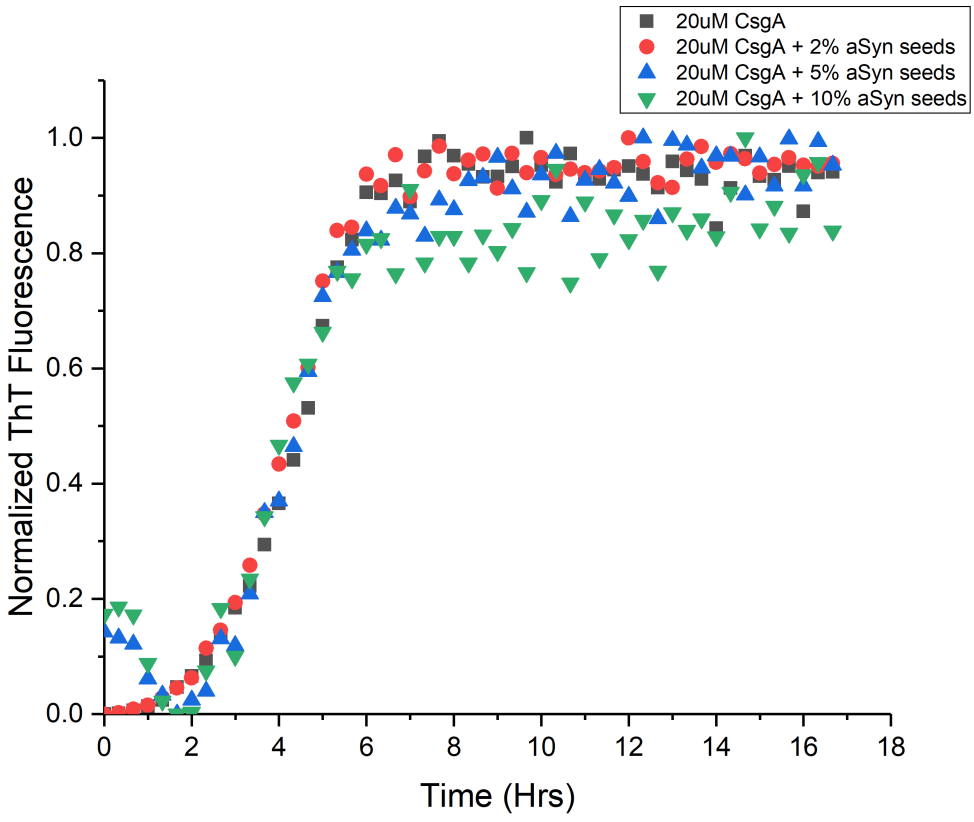

Figure 3.6: Preformed α-synuclein seeds had no effect on the rate of CsgA polymerization. Preformed α-synuclein seeds at concentrations of 2%, 5%, and 10% to of the CsgA concentration had no effect on the rate of CsgA polymerization.

forming over the course of an hour long experiment was achieved (Figure 3.10).

3.4 Conclusion

This data provided direct experimental evidence that CsgA and α-synuclein fibril formation can be directly visualized using this TIRF microscopy assay. This technique can therefore be used to study the kinetics of fibril assembly as well as a host of other unanswered questions regarding CsgA and α-synuclein cross-seeding such as; why soluable α-synulcein decreases the rate of fibril formation but preformed fibrils accelerate, do CsgA and α-synuclein form fibrils of mixed species

However, it is not yet well understood are how fibril formation is initiated nor how

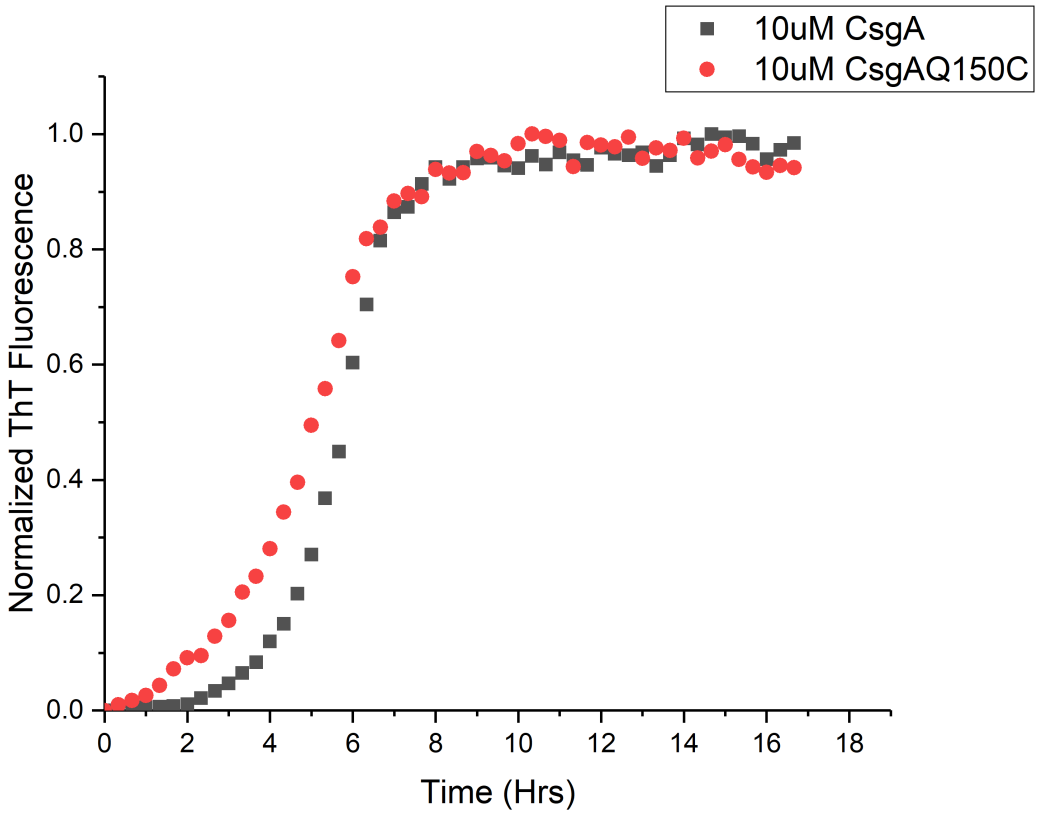

Figure 3.7: CsgA Q150C mutant kinetics do not significantly differ from those of WT CsgA. WT CsgA and Q150C fibril kinetics are comparable.

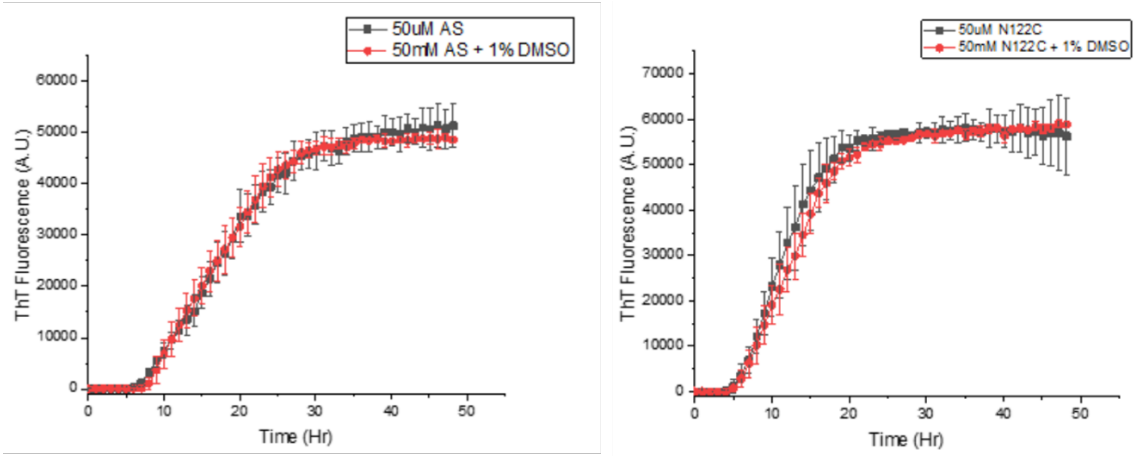

Figure 3.8: α-synuclein N122C did not significantly change kinetics of fibril formation. Polymerization of α-synuclein N122C and WT α-synuclein fibril formation kinetics were comparable as measured by ThT fluorescence assays.

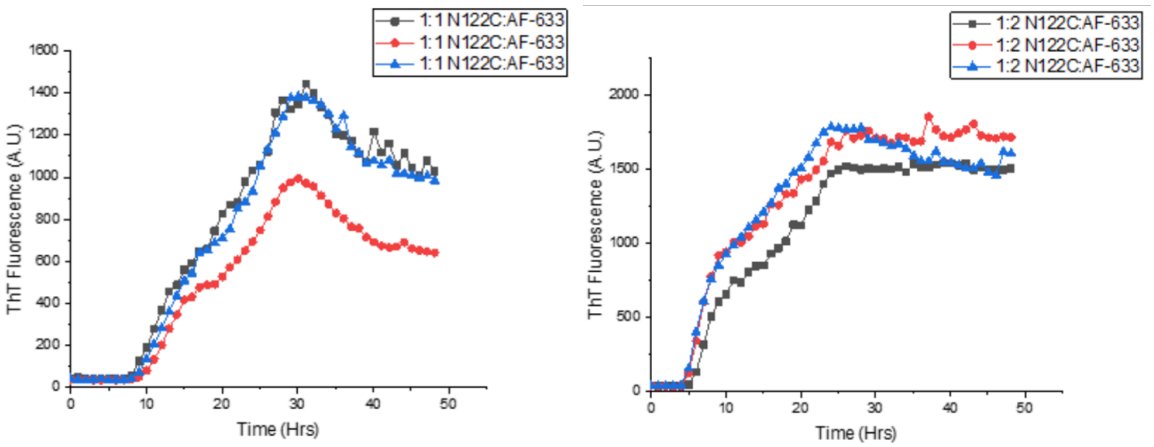

Figure 3.9: Addition of the AlexaFluor dye at high concentrations did have an affect kinetics of fibril formation. CsgA Q150C and at α-synuclein N122C labeled with high concentrations of AF-647 did have an affect kinetics of fibril formation.

fibrils can template further fibril polymerization.

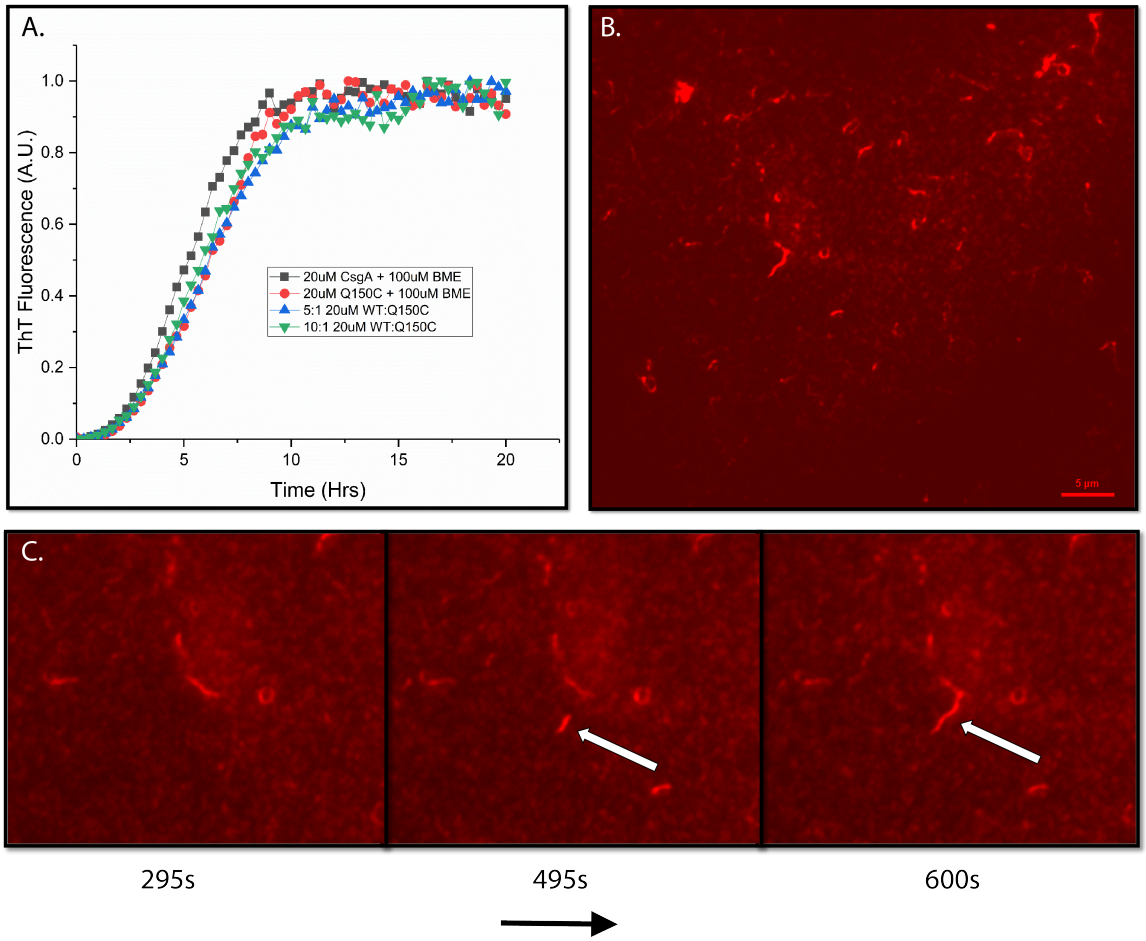

Figure 3.10: TIRF elongation assay of CsgA. Stills of CsgA elongating in a passivated culture well can be seen in the stills. The 10:1 molar ratio of CsgA was used. This ratio of labeled CsgA Q150C to WT unlabeled CsgA does not perturb kinetics of aggregation as measured by ThT (Panel A). TIRF elongation assay enables *in situ* measurement of the kinetics of fibril elongation.

CHAPTER IV

Ongoing and Future Directions

4.1 Introduction

Various proteins have been shown to inhibit the polymerization of another. For example, the human human systemic amyloid precursor protein transthyretin (TTR), which functions as a transportor theyroxine and retinol, has been shown to inhibit curli assembly [73]. Two other *E. coli* proteins in the curli secretion system, CsgC and CsgE, have both been shown to inhibit polymerization of CsgA both *in vitro* and *in vivo* [29, 43, 80, 133].

CsgC and CsgE have also been shown to decrease the rate of polymerization of α-synuclein. CsgC inhibits aSyn polymerization at a ratio as low as 1:100 presumably through interactions between an element of the aSyn sequence that is shared with CsgA [29, 43]. CsgE delays α-synuclein fibril formation at a molar ratio of 4:1. Several point mutants of CsgE were also made that were able to prolong the lag phase of aSyn relative to WT CsgE, but interestingly, these mutants were poor inhibitors of CsgA.

In addition to the natural modulators of fibril formation, chemical modulators of fibril formation have also been identified. The most potent inhibitor of CsgA inhibition identified thus far is the peptidomimetic ring-fused 2-pyridone molecule called FN075 (Figure 4.1) [6, 22]. FN075 has been shown to have differential effects on the aggregation of CsgA and α-synuclein [67]. Where FN075 promotes oligomerizatin of both proteins, α-synuclein oligomers are competent for amyloid formation while CsgA oligomers are not [67]. The

chemistry of 2-pyridone FN075 is well-established and highly-ameanable, diverse functional groups can be added as our understanding of structure function increases.

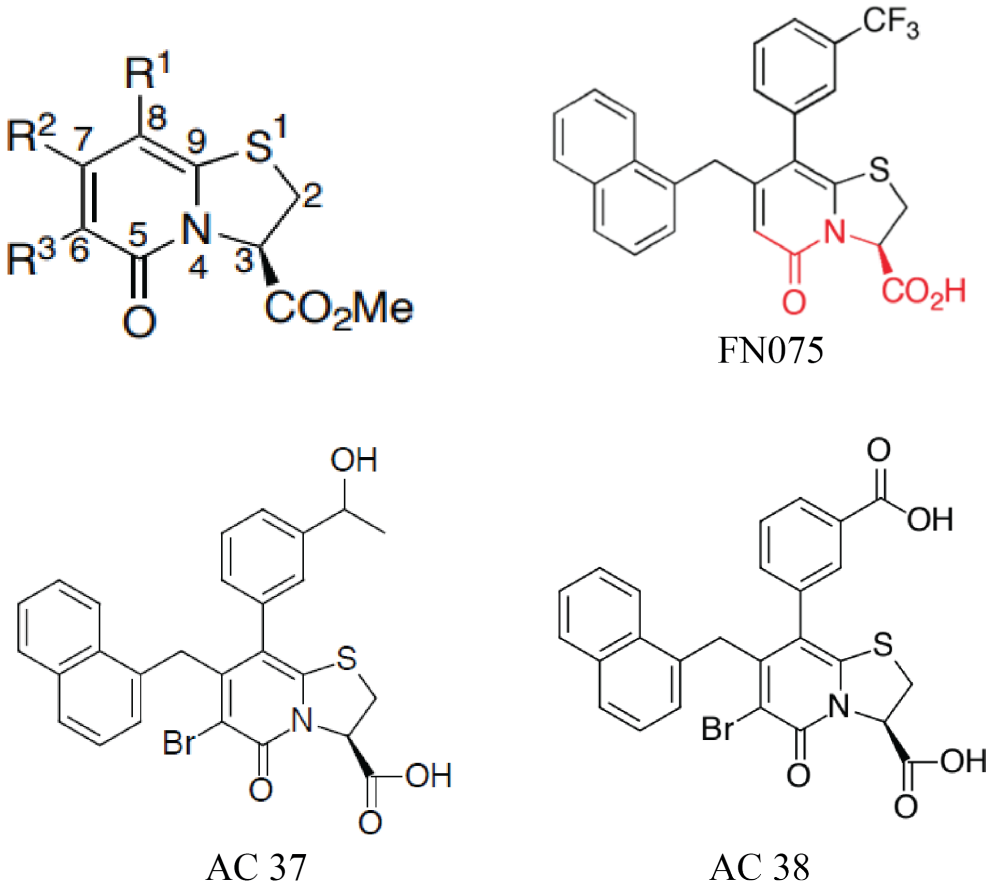

Figure 4.1: 2-pyridone amyloid inhibitors. The 2-pyridone scafford is shown with each of the modifiable sites highlighted. FN075 is the most potent CsgA inhibitor built on this scaffold. AC37 and AC38 illustrate the tunability of the molecule to gain further understanding of the structure-activity relationships.

4.2 Experimental procedures

4.2.1 Ion Mobility Mass Spectrometry

Proteins were prepared in a similar manner as for ThT assays without the addition of ThT (Chapter 3, Experimental procedures). Because of the large distribution of possible oligomeric species and limitations on the resolution capabilities of the instrument, protein samples were passed through 100 kDa cutoff coloumns to remove oligomers greater than

7-mers from the studies. Samples were then flash frozen at appropriate time points and passed off to the laboratory of Brandon Routolo for IMMS.

Refer to chapter 3 for further experimental proceducures.

4.3 Results

4.3.1 Initial screening of chemical modulators

As a high-throughput method of screening compounds, ThT assays were performed. CsgA and alpha-synuclein were purified into soluble monomers and allowed to incubate in the presence or absence of compound. At a fivefold molar excess (125 μM), FN075 has been shown to completely inhibit ThT fluorescence of 25μM CsgA over time (Cegelski et al., Nat Chem Bio 2009)(Figure 4.1).

It has previously been shown that the small molecule inhibitor FN075 inhibits fibril formation of the curli protein CsgA by promoting an off-pathway, non-amyloidogenic oligomer. FN075 also accelerates α-synuclein aggregation by stimulation the formation of on-pathway oligomer formation [67].

Though a great number of compounds were screened, very few of the compounds in the library screened so far have performed to the level of FN075 (Figure 4.2). Since all of the molecules are built off of the same scaffold with different chemical moieties decorating specific sites, substitutions will allow the investigation of structure-function relationships.

4.3.2 Ion mobility mass spectrometry shows that FN075 promotes an extended conformation

To identify the specific regions to which FN075 is binding, ion-mobility mass spectrometry was utilized (IMMS). IMMS is a powerful technique that enables the separation of complex mixtures [84]. It can be thought of as gas-phase electrophoresis. Specifically, this technique will be used to characterize the on-pathway oligomers formed immediately

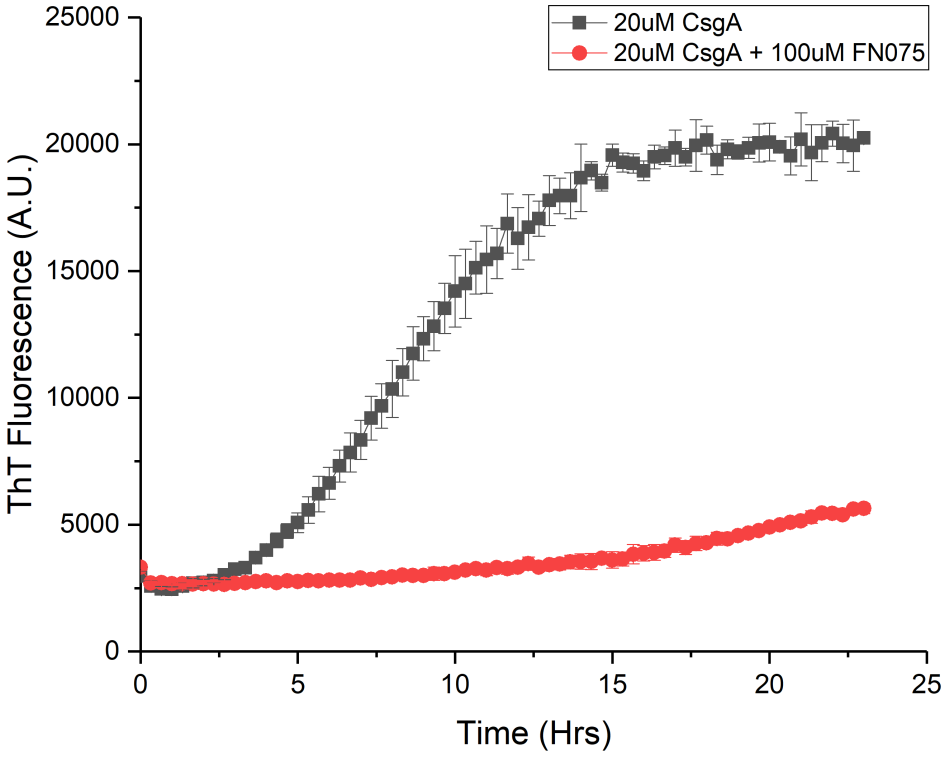

Figure 4.2: FN075 blocks fibril formation of CsgA and accelerates α-synuclein fibril formation. ThT fluorescence measurements of freshly purified CsgA with 20μM ThT measured at 15 minute intervals.

upon incubating the compound with alpha-synuclein.

Binding experiments were carried out to find out the number of alpha-synuclein subunits present in each oligomer and the number of bound FN075 molecules. The most interesting finding from these experiments thus far was that FN075 promotes a more extended conformation of monomeric alpha-synuclein (Figure 4.4). What was most surprising was that incubation of alpha-synuclein with FN075 resulted in a disappearance of dimer and higher order oligomeric peaks in the spectra (Figure 4.5). Reasons may be that the solvent required for IMMS experiments may be interfering with alpha-synuclein-FN075 oligomer assembly. Another reason may be that experiments are typically carried out at low temperatures and FN075 may not be stable. These are details that need to be figured out prior to continuation of this method to try to map the location of binding onto CsgA and alpha-

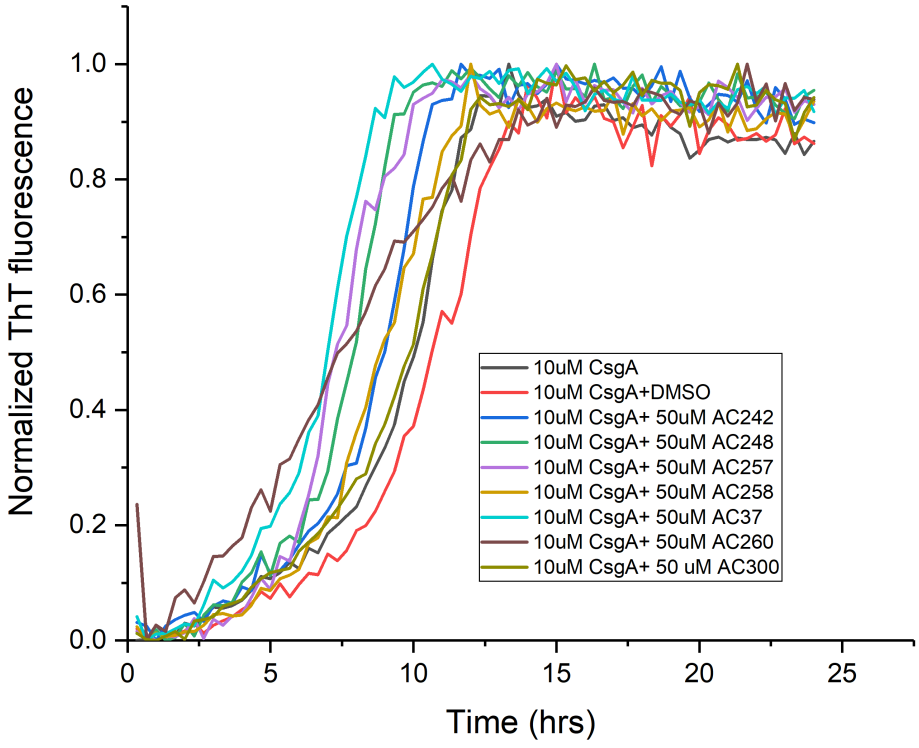

Figure 4.3: 2-pyridone compounds show a range of variability, however, no new potent inhibitor of CsgA has yet been identified. ThT fluorescence measurements of soluble CsgA incubated with 2-pyridone compounds at a 1:5 molar ratio excess.

synuclein.

Reasons may be that the solvent required for IMMS experiments may be interfering with alpha-synuclein-FN075 oligomer assembly. Another reason may be that experiments are typically carried out at low temperatures and FN075 may not be stable. These are details that need to be figured out prior to continuation of this method to try to map the location of binding onto CsgA and alpha-synuclein.

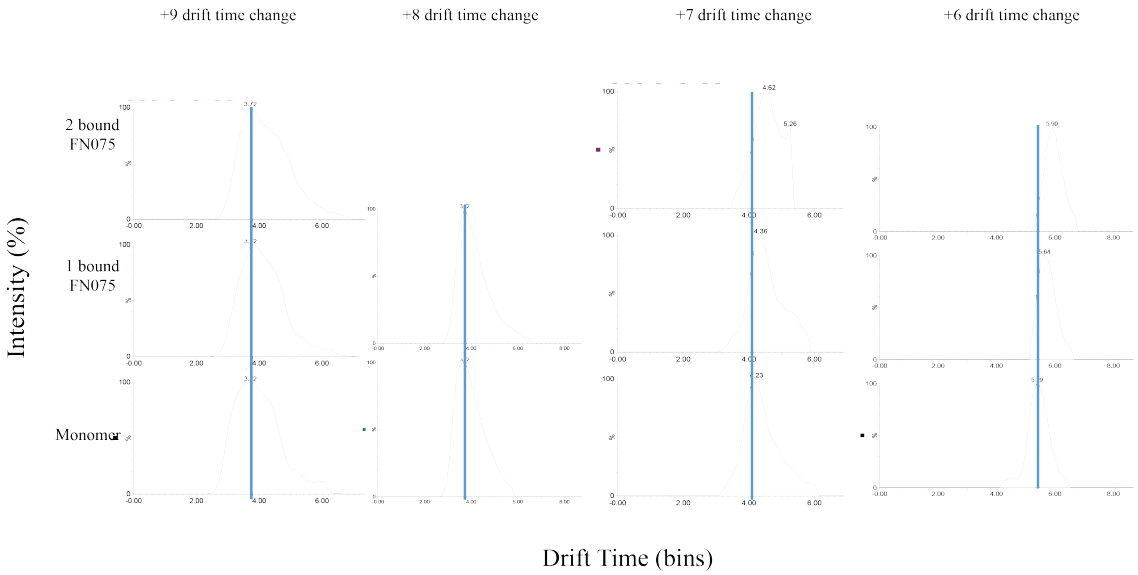

Figure 4.4: FN075 promotes a more extended α-synuclein monomer. Soluable α-synulcein incubated with FN075 at a 1:10 molar ratio indicates that FN075 promotes a more extended structure.

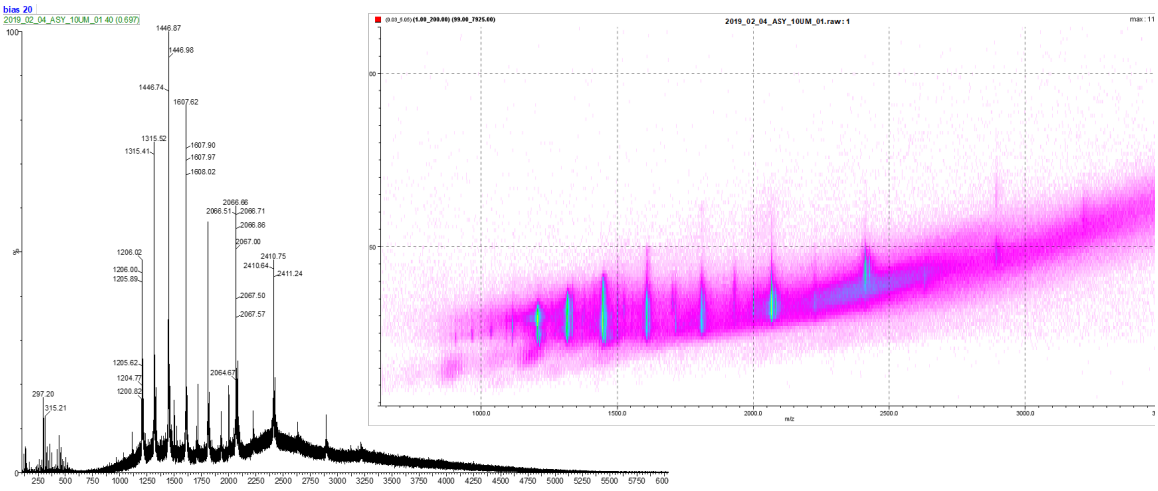

Figure 4.5: Soluble α-synuclein is predominantly made up of monomers and dimers. Soluable α-synuclein contains multiple ionization states of the protein in monomer and dimer states.

4.4 Conclusions

4.4.1 Cysteine biosynthesis metabolite inhibits biofilm formation

Bacteria living within biofilms are encapsulated in an extracellular matrix composed of proteins, exopolysaccharides, and DNA and many factors control the expression of the matrix components [**?**, 53, 92]. Curli are the major protein component of the E. coli extracellular matrix. Uropathogenic *E. coli* UTI89 can form pellicle biofilms in the lab, with curli

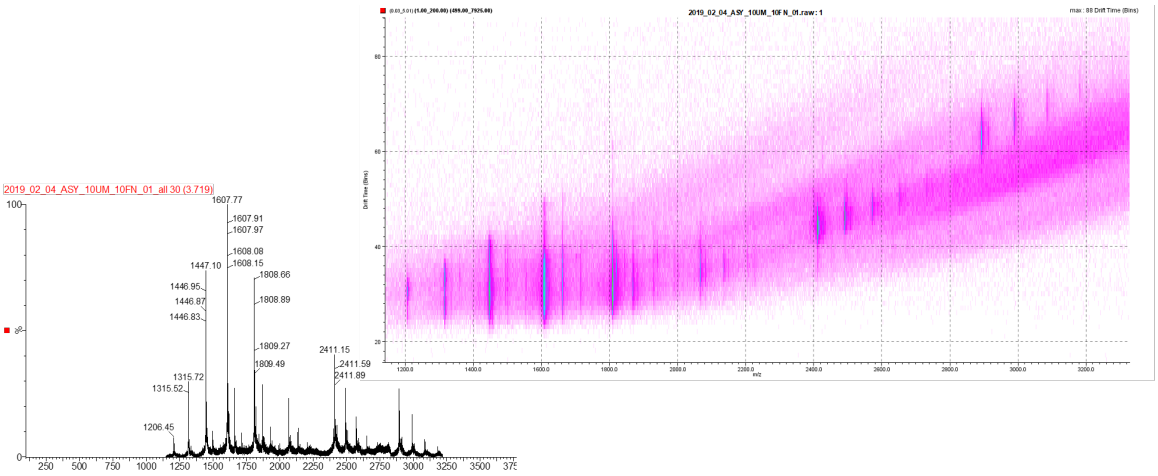

Figure 4.6: Soluble α-synuclein incubated with FN075 loses dimer species. α-synuclein incubated with FN075 at a 1:10 molar ratio (with FN075 in excess) indicates that FN075 causes a disappearance of the dimer species. Monomer compound complexes can be observed with 1-6 FN075 molecules bound.

being the major component. In Chapter 2, I found that aged UTI89 produces an antibiofilm inhibitor that inhibits its own pellicle formation. UTI89 grown in bacteria-free conditioned media was unable to form a pellicle biofilm. I was able to eliminate several molecular antibiofilm candidates. Along the way I was able to conclude that the antibiofilm activity was dependent on cysteine production as cysteine auxotrophs lost the ability to produce the biofilm inhibitor, and the phenotype could be complemented by addition of cysteine or cystine into mutant cultures. Though I am still unsure of how cysteine biosynthesis mediates the antibiofilm activity, there are a few hypotheses. One idea is that it may be a combination of many metabolic products may be combined to contribute the antibiofilm effect. Another idea that is worth exploring is the fact that YESCA media simply does not have enough tryptophan for the bacteria to efficiently convert to indole, a signaling molecule which has been shown to have antibiofilm effects.

4.4.2 TIRF microscopy can be used to measure fibril formation

In chapter 3, I showed that single-molecule TIRF experiments can be used to monitor fibril formation of CsgA and alpha-synuclein. We identified two CsgA and alpha-synuclein cysteine point mutants which behave wild type like in ThT assays and which can be

fluorescently tagged in TIRF experiments with AlexaFlour dyes for imaging. With a suite of maleimide dyes available, multi-color TIRF experiments can be executed to watch the interactions of CsgA and alpha-synulciein with fibers and monomers mixed in various combinations.

4.4.3 FN075 promotes an extended alpha-synuclein structure

In chapter 4, I showed that FN075 promotes a more extended monomer structure of alpha-synuclein. This illustrates that 2-pyridones coupled with IMMS are a powerful method of mapping the interactions of amyloid fibril formation with amyloids. Further, this illustrates that CsgA polymerization is a novel framework with which to assess the efficacy of drugs and other molecules to modulate amyloid fibril formation.

BIBLIOGRAPHY

BIBLIOGRAPHY

[1] Haley E Adcox, Erin M Vasicek, Varun Dwivedi, Ky V Hoang, Joanne Turner, and John S Gunn. Salmonella extracellular matrix components influence biofilm formation and gallbladder colonization. *Infection and immunity*, 84(11):3243–3251, 2016.

[2] Christian Beyschau Andersen, Hisashi Yagi, Mauro Manno, Vincenzo Martorana, Tadato Ban, Gunna Christiansen, Daniel Erik Otzen, Yuji Goto, and Christian Rischel. Branching in amyloid fibril growth. *Biophysical journal*, 96(4):1529–1536, 2009.

[3] GG Anderson and GA O'toole. Innate and induced resistance mechanisms of bacterial biofilms. In *Bacterial biofilms*, pages 85–105. Springer, 2008.

[4] Gregory G Anderson, Karen W Dodson, Thomas M Hooton, and Scott J Hultgren. Intracellular bacterial communities of uropathogenic escherichia coli in urinary tract pathogenesis. *Trends in microbiology*, 12(9):424–430, 2004.

[5] Gregory G Anderson, Joseph J Palermo, Joel D Schilling, Robyn Roth, John Heuser, and Scott J Hultgren. Intracellular bacterial biofilm-like pods in urinary tract infections. *Science*, 301(5629):105–107, 2003.

[6] Emma K Andersson, Christoffer Bengtsson, Margery L Evans, Erik Chorell, Magnus Sellstedt, Anders EG Lindgren, David A Hufnagel, Moumita Bhattacharya, Peter M Tessier, Pernilla Wittung-Stafshede, et al. Modulation of curli assembly and pellicle biofilm formation by chemical and protein chaperones. *Chemistry & biology*, 20(10):1245–1254, 2013.

[7] Paolo Arosio, Tuomas PJ Knowles, and Sara Linse. On the lag phase in amyloid fibril formation. *Physical Chemistry Chemical Physics*, 17(12):7606–7618, 2015.

[8] John W Austin, Greg Sanders, William W Kay, and S Karen Collinson. Thin aggregative fimbriae enhance salmonella enteritidis biofilm formation. *FEMS microbiology letters*, 162(2):295–301, 1998.

[9] N Awano, M Wada, A Kohdoh, T Oikawa, H Takagi, and S Nakamori. Effect of cysteine desulfhydrase gene disruption on l-cysteine overproduction in escherichia coli. *Applied microbiology and biotechnology*, 62(2-3):239–243, 2003.

[10] Naoki Awano, Masaru Wada, Hirotada Mori, Shigeru Nakamori, and Hiroshi Takagi. Identification and functional analysis of escherichia coli cysteine desulfhydrases. *Appl. Environ. Microbiol.*, 71(7):4149–4152, 2005.

[11] Fredrik Bäckhed, Ruth E Ley, Justin L Sonnenburg, Daniel A Peterson, and Jeffrey I Gordon. Host-bacterial mutualism in the human intestine. *science*, 307(5717):1915–1920, 2005.

[12] Tadato Ban, Daizo Hamada, Kazuhiro Hasegawa, Hironobu Naiki, and Yuji Goto. Direct observation of amyloid fibril growth monitored by thioflavin t fluorescence. *Journal of Biological Chemistry*, 278(19):16462–16465, 2003.

[13] Michelle M Barnhart and Matthew R Chapman. Curli biogenesis and function. *Annu. Rev. Microbiol.*, 60:131–147, 2006.

[14] Christophe Beloin, Agnès Roux, and J-M Ghigo. Escherichia coli biofilms. In *Bacterial Biofilms*, pages 249–289. Springer, 2008.

[15] S Bhoite, MR Chapman, H Remaut, et al. Curli biogenesis: Bacterial amyloid assembly by the type viii secretion pathway. *EcoSal Plus*, 8(2), 2019.

[16] Sylvain Bieler, Lisbell Estrada, Rosalba Lagos, Marcelo Baeza, Joaquín Castilla, and Claudio Soto. Amyloid formation modulates the biological activity of a bacterial protein. *Journal of Biological Chemistry*, 280(29):26880–26885, 2005.

[17] Luz P Blanco, Margery L Evans, Daniel R Smith, Matthew P Badtke, and Matthew R Chapman. Diversity, biogenesis and function of microbial amyloids. *Trends in microbiology*, 20(2):66–73, 2012.

[18] Zachary D Blount. The natural history of model organisms: The unexhausted potential of e. coli. *Elife*, 4:e05826, 2015.

[19] Blaise R Boles and Alexander R Horswill. Staphylococcal biofilm disassembly. *Trends in microbiology*, 19(9):449–455, 2011.

[20] Steven S Branda, Åshild Vik, Lisa Friedman, and Roberto Kolter. Biofilms: the matrix revisited. *Trends in microbiology*, 13(1):20–26, 2005.

[21] Baohua Cao, Yan Zhao, Yongjun Kou, Dongchun Ni, Xuejun Cai Zhang, and Yihua Huang. Structure of the nonameric bacterial amyloid secretion channel. *Proceedings of the National Academy of Sciences*, 111(50):E5439–E5444, 2014.

[22] Lynette Cegelski, Jerome S Pinkner, Neal D Hammer, Corinne K Cusumano, Chia S Hung, Erik Chorell, Veronica Åberg, Jennifer N Walker, Patrick C Seed, Fredrik Almqvist, et al. Small-molecule inhibitors target escherichia coli amyloid biogenesis and biofilm formation. *Nature chemical biology*, 5(12):913, 2009.

[23] Matthew R Chapman, Lloyd S Robinson, Jerome S Pinkner, Robyn Roth, John Heuser, Mårten Hammar, Staffan Normark, and Scott J Hultgren. Role of escherichia coli curli operons in directing amyloid fiber formation. *Science*, 295(5556):851–855, 2002.

[24] Shu G Chen, Vilius Stribinskis, Madhavi J Rane, Donald R Demuth, Evelyne Gozal, Andrew M Roberts, Rekha Jagadapillai, Ruolan Liu, Kyonghwan Choe, Bhooma Shivakumar, et al. Exposure to the functional bacterial amyloid protein curli enhances alpha-synuclein aggregation in aged fischer 344 rats and caenorhabditis elegans. *Scientific reports*, 6:34477, 2016.

[25] Swaine L Chen, Chia-Seui Hung, Jian Xu, Christopher S Reigstad, Vincent Magrini, Aniko Sabo, Darin Blasiar, Tamberlyn Bieri, Rekha R Meyer, Philip Ozersky, et al. Identification of genes subject to positive selection in uropathogenic strains of escherichia coli: a comparative genomics approach. *Proceedings of the National Academy of Sciences*, 103(15):5977–5982, 2006.

[26] Izhack Cherny, Liat Rockah, Orlev Levy-Nissenbaum, Uri Gophna, Eliora Z Ron, and Ehud Gazit. The formation of escherichia coli curli amyloid fibrils is mediated by prion-like peptide repeats. *Journal of molecular biology*, 352(2):245–252, 2005.

[27] Fabrizio Chiti and Christopher M Dobson. Protein misfolding, functional amyloid, and human disease. *Annu. Rev. Biochem.*, 75:333–366, 2006.

[28] Fabrizio Chiti and Christopher M Dobson. Protein misfolding, amyloid formation, and human disease: a summary of progress over the last decade. *Annual review of biochemistry*, 86:27–68, 2017.

[29] Erik Chorell, Emma Andersson, Margery L Evans, Neha Jain, Anna Götheson, Jörgen Åden, Matthew R Chapman, Fredrik Almqvist, and Pernilla Wittung-Stafshede. Bacterial chaperones csge and csgc differentially modulate human α-synuclein amyloid formation via transient contacts. *PloS one*, 10(10):e0140194, 2015.

[30] SK Collinson, PC Doig, JL Doran, S Clouthier, WW Kay, et al. Thin, aggregative fimbriae mediate binding of salmonella enteritidis to fibronectin. *Journal of bacteriology*, 175(1):12–18, 1993.

[31] Tobias Daßler, Thomas Maier, Christoph Winterhalter, and August Böck. Identification of a major facilitator protein from escherichia coli involved in efflux of metabolites of the cysteine pathway. *Molecular microbiology*, 36(5):1101–1112, 2000.

[32] Kirill A Datsenko and Barry L Wanner. One-step inactivation of chromosomal genes in escherichia coli k-12 using pcr products. *Proceedings of the National Academy of Sciences*, 97(12):6640–6645, 2000.

[33] Mary Ellen Davey and George A O'toole. Microbial biofilms: from ecology to molecular genetics. *Microbiol. Mol. Biol. Rev.*, 64(4):847–867, 2000.

[34] Erwin J De Genst, Tim Guilliams, Joke Wellens, Elizabeth M O'Day, Christopher A Waudby, Sarah Meehan, Mireille Dumoulin, Shang-Te Danny Hsu, Nunilo Cremades, Koen HG Verschueren, et al. Structure and properties of a complex of α-synuclein and a single-domain camelid antibody. *Journal of molecular biology*, 402(2):326–343, 2010.

[35] Eugene A Delwiche. Activators for the cysteine desulfhydrase system of an escherichia coli mutant. *Journal of bacteriology*, 62(6):717, 1951.

[36] William H DePas, David A Hufnagel, John S Lee, Luz P Blanco, Hans C Bernstein, Steve T Fisher, Garth A James, Philip S Stewart, and Matthew R Chapman. Iron induces bimodal population development by escherichia coli. *Proceedings of the National Academy of Sciences*, 110(7):2629–2634, 2013.

[37] Maya Deshmukh, Margery L Evans, and Matthew R Chapman. Amyloid by design: intrinsic regulation of microbial amyloid assembly. *Journal of molecular biology*, 430(20):3631–3641, 2018.

[38] Joanna Domka, Jintae Lee, Tarun Bansal, and Thomas K Wood. Temporal gene-expression in escherichia coli k-12 biofilms. *Environmental microbiology*, 9(2):332–346, 2007.

[39] David Eisenberg and Mathias Jucker. The amyloid state of proteins in human diseases. *Cell*, 148(6):1188–1203, 2012.

[40] Marie A Elliot, Nitsara Karoonuthaisiri, Jianqiang Huang, Maureen J Bibb, Stanley N Cohen, Camilla M Kao, and Mark J Buttner. The chaplins: a family of hydrophobic cell-surface proteins involved in aerial mycelium formation in streptomyces coelicolor. *Genes & development*, 17(14):1727–1740, 2003.

[41] Elisabeth Ashman Epstein, Margeaux A Reizian, and Matthew R Chapman. Spatial clustering of the curlin secretion lipoprotein requires curli fiber assembly. *Journal of bacteriology*, 191(2):608–615, 2009.

[42] Margery L Evans and Matthew R Chapman. Curli biogenesis: order out of disorder. *Biochimica et Biophysica Acta (BBA)-Molecular Cell Research*, 1843(8):1551–1558, 2014.

[43] Margery L Evans, Erik Chorell, Jonathan D Taylor, Jörgen Åden, Anna Götheson, Fei Li, Marion Koch, Lea Sefer, Steve J Matthews, Pernilla Wittung-Stafshede, et al. The bacterial curli system possesses a potent and selective inhibitor of amyloid formation. *Molecular cell*, 57(3):445–455, 2015.

[44] Margery L Evans, Elizabeth Gichana, Yizhou Zhou, and Matthew R Chapman. Bacterial amyloids. In *Amyloid Proteins*, pages 267–288. Springer, 2018.

[45] Jesper Ferkinghoff-Borg, Jesper Fonslet, Christian Beyschau Andersen, Sandeep Krishna, Simone Pigolotti, Hisashi Yagi, Yuji Goto, Daniel Otzen, and Mogens H Jensen. Stop-and-go kinetics in amyloid fibrillation. *Physical Review E*, 82(1):010901, 2010.

[46] Hans-Curt Flemming and Jost Wingender. The biofilm matrix. *Nature reviews microbiology*, 8(9):623, 2010.

[47] Dennis H Flint, Joseph F Tuminello, and Thomas J Miller. Studies on the synthesis of the fe-s cluster of dihydroxy-acid dehydratase in escherichia coli crude extract isolation of o-acetylserine sulfhydrylases a and b and β-cystathionase based on their ability to mobilize sulfur from cysteine and to participate in fe-s cluster synthesis. *Journal of Biological Chemistry*, 271(27):16053–16067, 1996.

[48] Douglas M Fowler, Atanas V Koulov, Christelle Alory-Jost, Michael S Marks, William E Balch, and Jeffery W Kelly. Functional amyloid formation within mammalian tissue. *PLoS biology*, 4(1):e6, 2005.

[49] Betsy Foxman. The epidemiology of urinary tract infection. *Nature Reviews Urology*, 7(12):653, 2010.

[50] Isabel Franke, Armin Resch, Tobias Daßler, Thomas Maier, and August Böck. Yfik from escherichia coli promotes export of o-acetylserine and cysteine. *Journal of bacteriology*, 185(4):1161–1166, 2003.

[51] Robert P Friedland and Matthew R Chapman. The role of microbial amyloid in neurodegeneration. *PLoS pathogens*, 13(12):e1006654, 2017.

[52] Paul M Gallo, Glenn J Rapsinski, R Paul Wilson, Gertrude O Oppong, Uma Sriram, Mark Goulian, Bettina Buttaro, Roberto Caricchio, Stefania Gallucci, and Çagla Tükel. Amyloid-dna composites of bacterial biofilms stimulate autoimmunity. *Immunity*, 42(6):1171–1184, 2015.

[53] Ulrich Gerstel and Ute Römling. Oxygen tension and nutrient starvation are major signals that regulate agfd promoter activity and expression of the multicellular morphotype in salmonella typhimurium. *Environmental microbiology*, 3(10):638–648, 2001.

[54] Peter Gilbert, Tomas Maira-Litran, Andrew J McBain, Alexander H Rickard, and Fraser W Whyte. The physiology and collective recalcitrance of microbial biofilm communities. *Advances in microbial physiology*, 46:202–256, 2002.

[55] George G Glenner and Caine W Wong. Alzheimer's disease: initial report of the purification and characterization of a novel cerebrovascular amyloid protein. *Biochemical and biophysical research communications*, 120(3):885–890, 1984.

[56] U Gophna, M Barlev, R Seijffers, TA Oelschlager, J Hacker, and EZ Ron. Curli fibers mediate internalization ofescherichia coli by eukaryotic cells. *Infection and immunity*, 69(4):2659–2665, 2001.

[57] Uri Gophna, Tobias A Oelschlaeger, Joerg Hacker, and Eliora Z Ron. Role of fibronectin in curli-mediated internalization. *FEMS microbiology letters*, 212(1):55–58, 2002.

[58] Parveen Goyal, Petya V Krasteva, Nani Van Gerven, Francesca Gubellini, Imke Van den Broeck, Anastassia Troupiotis-Tsaïlaki, Wim Jonckheere, Gérard Péhau-Arnaudet, Jerome S Pinkner, Matthew R Chapman, et al. Structural and mechanistic

insights into the bacterial amyloid secretion channel csgg. *Nature*, 516(7530):250, 2014.

[59] Maria Hadjifrangiskou, Alice P Gu, Jerome S Pinkner, Maria Kostakioti, Ellisa W Zhang, Sarah E Greene, and Scott J Hultgren. Transposon mutagenesis identifies uropathogenic escherichia coli biofilm factors. *Journal of bacteriology*, 194(22):6195–6205, 2012.

[60] Luanne Hall-Stoodley, J William Costerton, and Paul Stoodley. Bacterial biofilms: from the natural environment to infectious diseases. *Nature reviews microbiology*, 2(2):95, 2004.

[61] Luanne Hall-Stoodley and Paul Stoodley. Evolving concepts in biofilm infections. *Cellular microbiology*, 11(7):1034–1043, 2009.

[62] M» rten Hammar, Anna Arnqvist, Zhao Bian, Arne Olsén, and Staffan Normark. Expression of two csg operons is required for production of fibronectin-and congo red-binding curli polymers in escherichia coli k-12. *Molecular microbiology*, 18(4):661–670, 1995.

[63] Brian K Hammer and Bonnie L Bassler. Quorum sensing controls biofilm formation in vibrio cholerae. *Molecular microbiology*, 50(1):101–104, 2003.

[64] Neal D Hammer, Bryan A McGuffie, Yizhou Zhou, Matthew P Badtke, Ashley A Reinke, Kristoffer Brännström, Jason E Gestwicki, Anders Olofsson, Fredrik Almqvist, and Matthew R Chapman. The c-terminal repeating units of csgb direct bacterial functional amyloid nucleation. *Journal of molecular biology*, 422(3):376–389, 2012.

[65] Neal D Hammer, Jens C Schmidt, and Matthew R Chapman. The curli nucleator protein, csgb, contains an amyloidogenic domain that directs csga polymerization. *Proceedings of the National Academy of Sciences*, 104(30):12494–12499, 2007.

[66] Niels Høiby, Thomas Bjarnsholt, Michael Givskov, Søren Molin, and Oana Ciofu. Antibiotic resistance of bacterial biofilms. *International journal of antimicrobial agents*, 35(4):322–332, 2010.

[67] Istvan Horvath, Christoph F Weise, Emma K Andersson, Erik Chorell, Magnus Sellstedt, Christoffer Bengtsson, Anders Olofsson, Scott J Hultgren, Matthew Chapman, Magnus Wolf-Watz, et al. Mechanisms of protein oligomerization: inhibitor of functional amyloids templates α-synuclein fibrillation. *Journal of the American Chemical Society*, 134(7):3439–3444, 2012.

[68] Wenmao Huang, Xin Wu, Xiang Gao, Yifei Yu, Hai Lei, Zhenshu Zhu, Yi Shi, Yulan Chen, Meng Qin, Wei Wang, et al. Maleimide–thiol adducts stabilized through stretching. *Nature chemistry*, 11(4):310, 2019.

[69] David A Hufnagel, William H DePas, and Matthew R Chapman. The disulfide bonding system suppresses csgd-independent cellulose production in escherichia coli. *Journal of bacteriology*, 196(21):3690–3699, 2014.

[70] David A Hufnagel, Janet E Price, Rachel E Stephenson, Jesse Kelley, Matthew F Benoit, and Matthew R Chapman. Thiol starvation induces redox-mediated dysregulation of escherichia coli biofilm components. *Journal of bacteriology*, 200(1):e00389–17, 2018.

[71] David A Hufnagel, Çagla Tükel, and Matthew R Chapman. Disease to dirt: the biology of microbial amyloids. *PLoS pathogens*, 9(11):e1003740, 2013.

[72] Chia Hung, Yizhou Zhou, Jerome S Pinkner, Karen W Dodson, Jan R Crowley, John Heuser, Matthew R Chapman, Maria Hadjifrangiskou, Jeffrey P Henderson, and Scott J Hultgren. Escherichia coli biofilms have an organized and complex extracellular matrix structure. *MBio*, 4(5):e00645–13, 2013.

[73] Neha Jain, Jörgen Ådén, Kanna Nagamatsu, Margery L Evans, Xinyi Li, Brennan McMichael, Magdalena I Ivanova, Fredrik Almqvist, Joel N Buxbaum, and Matthew R Chapman. Inhibition of curli assembly and escherichia coli biofilm formation by the human systemic amyloid precursor transthyretin. *Proceedings of the National Academy of Sciences*, 114(46):12184–12189, 2017.

[74] Jeonghwan Jang, H-G Hur, Michael J Sadowsky, MN Byappanahalli, Tao Yan, and Satoshi Ishii. Environmental escherichia coli: ecology and public health implications—a review. *Journal of applied microbiology*, 123(3):570–581, 2017.

[75] Cecilia Johansson, Therese Nilsson, Arne Olsén, and Mary Jo Wick. The influence of curli, a mhc-i-binding bacterial surface structure, on macrophage—t cell interactions. *FEMS Immunology & Medical Microbiology*, 30(1):21–29, 2001.

[76] Kristina Jonas, Henrik Tomenius, Abdul Kader, Staffan Normark, Ute Römling, Lyubov M Belova, and Öjar Melefors. Roles of curli, cellulose and bapa in salmonella biofilm morphology studied by atomic force microscopy. *BMC microbiology*, 7(1):70, 2007.

[77] Rolf S Kaas, Carsten Friis, David W Ussery, and Frank M Aarestrup. Estimating variation within the genes and inferring the phylogeny of 186 sequenced diverse escherichia coli genomes. *BMC genomics*, 13(1):577, 2012.

[78] Gabriele S Kaminski Schierle, Sebastian Van De Linde, Miklos Erdelyi, Elin K Esbjorner, Teresa Klein, Eric Rees, Carlos W Bertoncini, Christopher M Dobson, Markus Sauer, and Clemens F Kaminski. In situ measurements of the formation and morphology of intracellular β-amyloid fibrils by super-resolution fluorescence imaging. *Journal of the American Chemical Society*, 133(33):12902–12905, 2011.

[79] Ece Karatan and Paula Watnick. Signals, regulatory networks, and materials that build and break bacterial biofilms. *Microbiol. Mol. Biol. Rev.*, 73(2):310–347, 2009.

[80] Roger D Klein, Qin Shu, Zachary T Cusumano, Kanna Nagamatsu, Nathaniel C Gualberto, Aaron JL Lynch, Chao Wu, Wenjie Wang, Neha Jain, Jerome S Pinkner, et al. Structure-function analysis of the curli accessory protein csge defines surfaces essential for coordinating amyloid fiber formation. *MBio*, 9(4):e01349–18, 2018.

[81] Ilana Kolodkin-Gal, Diego Romero, Shugeng Cao, Jon Clardy, Roberto Kolter, and Richard Losick. D-amino acids trigger biofilm disassembly. *Science*, 328(5978):627–629, 2010.

[82] Nicholas M Kredich and Gordon M Tomkins. The enzymic synthesis of l-cysteine in escherichia coli and salmonella typhimurium. *Journal of Biological Chemistry*, 241(21):4955–4965, 1966.

[83] Pascal Kuner, Bernd Bohrmann, Lars O Tjernberg, Jan Näslund, Gerda Huber, Suna Celenk, Fiona Grüninger-Leitch, J Grayson Richards, Roland Jakob-Rœtne, John A Kemp, et al. Controlling polymerization of β-amyloid and prion-derived peptides with synthetic small molecule ligands. *Journal of Biological Chemistry*, 275(3):1673–1678, 2000.

[84] Francesco Lanucara, Stephen W Holman, Christopher J Gray, and Claire E Eyers. The power of ion mobility-mass spectrometry for structural characterization and the study of conformational dynamics. *Nature chemistry*, 6(4):281, 2014.

[85] Poul Larsen, Jeppe Lund Nielsen, Morten Simonsen Dueholm, Ronald Wetzel, Daniel Otzen, and Per Halkjær Nielsen. Amyloid adhesins are abundant in natural biofilms. *Environmental microbiology*, 9(12):3077–3090, 2007.

[86] Jintae Lee, Arul Jayaraman, and Thomas K Wood. Indole is an inter-species biofilm signal mediated by sdia. *BMC microbiology*, 7(1):42, 2007.

[87] Jintae Lee, Xue-Song Zhang, Manjunath Hegde, William E Bentley, Arul Jayaraman, and Thomas K Wood. Indole cell signaling occurs primarily at low temperatures in escherichia coli. *The ISME journal*, 2(10):1007, 2008.

[88] Ji Youn Lim, Janine M May, and Lynette Cegelski. Dimethyl sulfoxide and ethanol elicit increased amyloid biogenesis and amyloid-integrated biofilm formation in escherichia coli. *Appl. Environ. Microbiol.*, 78(9):3369–3378, 2012.

[89] Hannes Loferer, Mårten Hammar, and Staffan Normark. Availability of the fibre subunit csga and the nucleator protein csgb during assembly of fibronectin-binding curli is limited by the intracellular concentration of the novel lipoprotein csgg. *Molecular microbiology*, 26(1):11–23, 1997.

[90] Katarzyna Lundmark, Gunilla T Westermark, Arne Olsén, and Per Westermark. Protein fibrils in nature can enhance amyloid protein a amyloidosis in mice: Cross-seeding as a disease mechanism. *Proceedings of the National Academy of Sciences*, 102(17):6098–6102, 2005.

[91] Thien-Fah C Mah and George A O'Toole. Mechanisms of biofilm resistance to antimicrobial agents. *Trends in microbiology*, 9(1):34–39, 2001.

[92] John J Maurer, Thomas P Brown, WL Steffens, and Stephan G Thayer. The occurrence of ambient temperature-regulated adhesins, curli, and the temperature-sensitive hemagglutinin tsh among avian escherichia coli. *Avian diseases*, 42(1):106–118, 1998.

[93] MA Metaxas and EA Delwiche. The l-cysteine desulfhydrase of escherichia coli. *Journal of bacteriology*, 70(6):735, 1955.

[94] Matthew A Mulvey, Joel D Schilling, and Scott J Hultgren. Establishment of a persistent escherichia coli reservoir during the acute phase of a bladder infection. *Infection and immunity*, 69(7):4572–4579, 2001.

[95] Shigeru Nakamori, Shin-ichiro Kobayashi, Chitose Kobayashi, and Hiroshi Takagi. Overproduction of l-cysteine andl-cystine by escherichia coli strains with a genetically altered serine acetyltransferase. *Appl. Environ. Microbiol.*, 64(5):1607–1611, 1998.

[96] Rebecca Nelson, Michael R Sawaya, Melinda Balbirnie, Anders Ø Madsen, Christian Riekel, Robert Grothe, and David Eisenberg. Structure of the cross-β spine of amyloid-like fibrils. *Nature*, 435(7043):773, 2005.

[97] Ashley A Nenninger, Lloyd S Robinson, and Scott J Hultgren. Localized and efficient curli nucleation requires the chaperone-like amyloid assembly protein csgf. *Proceedings of the National Academy of Sciences*, 106(3):900–905, 2009.

[98] Hiroshi Ogasawara, Kaneyoshi Yamamoto, and Akira Ishihama. Role of the biofilm master regulator csgd in cross-regulation between biofilm formation and flagellar synthesis. *Journal of bacteriology*, 193(10):2587–2597, 2011.

[99] Iwao Ohtsu, Natthawut Wiriyathanawudhiwong, Susumu Morigasaki, Takeshi Nakatani, Hiroshi Kadokura, and Hiroshi Takagi. The l-cysteine/l-cystine shuttle system provides reducing equivalents to the periplasm in escherichia coli. *Journal of Biological Chemistry*, 285(23):17479–17487, 2010.

[100] A Olsen, Anna Arnqvist, M Hammar, and S Normark. Environmental regulation of curli production in escherichia coli. *Infectious agents and disease*, 2(4):272–274, 1993.

[101] Okako Omadjela, Adishesh Narahari, Joanna Strumillo, Hugo Mélida, Olga Mazur, Vincent Bulone, and Jochen Zimmer. Bcsa and bcsb form the catalytically active core of bacterial cellulose synthase sufficient for in vitro cellulose synthesis. *Proceedings of the National Academy of Sciences*, 110(44):17856–17861, 2013.

[102] Brian O'Nuallain, Shankaramma Shivaprasad, Indu Kheterpal, and Ronald Wetzel. Thermodynamics of aβ (1- 40) amyloid fibril elongation. *Biochemistry*, 44(38):12709–12718, 2005.

[103] Tslil Ophir and David L Gutnick. A role for exopolysaccharides in the protection of microorganisms from desiccation. *Appl. Environ. Microbiol.*, 60(2):740–745, 1994.

[104] Gertrude O Oppong, Glenn J Rapsinski, Tiffanny N Newman, Jessalyn H Nishimori, Steven G Biesecker, and Çagla Tükel. Epithelial cells augment barrier function via activation of the toll-like receptor 2/phosphatidylinositol 3-kinase pathway upon recognition of salmonella enterica serovar typhimurium curli fibrils in the gut. *Infection and immunity*, 81(2):478–486, 2013.

[105] Angel Orte, Neil R Birkett, Richard W Clarke, Glyn L Devlin, Christopher M Dobson, and David Klenerman. Direct characterization of amyloidogenic oligomers by single-molecule fluorescence. *Proceedings of the National Academy of Sciences*, 105(38):14424–14429, 2008.

[106] George O'Toole, Heidi B Kaplan, and Roberto Kolter. Biofilm formation as microbial development. *Annual Reviews in Microbiology*, 54(1):49–79, 2000.

[107] JA Otter, Karen Vickery, JT d Walker, E deLancey Pulcini, Paul Stoodley, SD Goldenberg, JAG Salkeld, J Chewins, S Yezli, and JD Edgeworth. Surface-attached cells, biofilms and biocide susceptibility: implications for hospital cleaning and disinfection. *Journal of Hospital Infection*, 89(1):16–27, 2015.

[108] Sunny Park and James A Imlay. High levels of intracellular cysteine promote oxidative dna damage by driving the fenton reaction. *Journal of bacteriology*, 185(6):1942–1950, 2003.

[109] Dorothea Pinotsi, Alexander K Buell, Celine Galvagnion, Christopher M Dobson, Gabriele S Kaminski Schierle, and Clemens F Kaminski. Direct observation of heterogeneous amyloid fibril growth kinetics via two-color super-resolution microscopy. *Nano letters*, 14(1):339–345, 2013.

[110] Claire Prigent-Combaret, Eva Brombacher, Olivier Vidal, Arnaud Ambert, Philippe Lejeune, Paolo Landini, and Corinne Dorel. Complex regulatory network controls initial adhesion and biofilm formation in escherichia coli via regulation of thecsgd gene. *Journal of bacteriology*, 183(24):7213–7223, 2001.

[111] Claire Prigent-Combaret, Gérard Prensier, Thanh Thuy Le Thi, Olivier Vidal, Philippe Lejeune, and Corinne Dorel. Developmental pathway for biofilm formation in curli-producing escherichia coli strains: role of flagella, curli and colanic acid. *Environmental microbiology*, 2(4):450–464, 2000.

[112] Richard A Proctor, Christof Von Eiff, Barbara C Kahl, Karsten Becker, Peter McNamara, Mathias Herrmann, and Georg Peters. Small colony variants: a pathogenic form of bacteria that facilitates persistent and recurrent infections. *Nature Reviews Microbiology*, 4(4):295, 2006.

[113] Peramaiyan Rajendran, Thamaraiselvan Rengarajan, Jayakumar Thangavel, Yutaka Nishigaki, Dhanapal Sakthisekaran, Gautam Sethi, and Ikuo Nishigaki. The vascular endothelium and human diseases. *International journal of biological sciences*, 9(10):1057, 2013.

[114] Glenn J Rapsinski, Meghan A Wynosky-Dolfi, Gertrude O Oppong, Sarah A Tursi, R Paul Wilson, Igor E Brodsky, and Çagla Tükel. Toll-like receptor 2 and nlrp3 cooperate to recognize a functional bacterial amyloid, curli. *Infection and immunity*, 83(2):693–701, 2015.

[115] Courtney Reichhardt and Lynette Cegelski. Solid-state nmr for bacterial biofilms. *Molecular physics*, 112(7):887–894, 2014.

[116] Olaya Rendueles, Jeffrey B Kaplan, and Jean-Marc Ghigo. Antibiofilm polysaccharides. *Environmental microbiology*, 15(2):334–346, 2013.

[117] Lloyd S Robinson, Elisabeth M Ashman, Scott J Hultgren, and Matthew R Chapman. Secretion of curli fibre subunits is mediated by the outer membrane-localized csgg protein. *Molecular microbiology*, 59(3):870–881, 2006.

[118] Diego Romero, Claudio Aguilar, Richard Losick, and Roberto Kolter. Amyloid fibers provide structural integrity to bacillus subtilis biofilms. *Proceedings of the National Academy of Sciences*, 107(5):2230–2234, 2010.

[119] Ute Römling, Zhao Bian, Mårten Hammar, Walter D Sierralta, and Staffan Normark. Curli fibers are highly conserved between salmonella typhimurium and escherichia coli with respect to operon structure and regulation. *Journal of bacteriology*, 180(3):722–731, 1998.

[120] Ute Römling, Manfred Rohde, Arne Olsén, Staffan Normark, and Jürgen Reinköster. Agfd, the checkpoint of multicellular and aggregative behaviour in salmonella typhimurium regulates at least two independent pathways. *Molecular microbiology*, 36(1):10–23, 2000.

[121] Christopher A Ross and Michelle A Poirier. Protein aggregation and neurodegenerative disease. *Nature medicine*, 10(7s):S10, 2004.

[122] Agnieszka Sekowska, Hsiang-Fu Kung, Antoine Danchin, et al. Sulfur metabolism in escherichia coli and related bacteria: facts and fiction. *Journal of molecular microbiology and biotechnology*, 2(2):145–177, 2000.

[123] Tricia R Serio, Anil G Cashikar, Anthony S Kowal, George J Sawicki, Jahan J Moslehi, Louise Serpell, Morton F Arnsdorf, and Susan L Lindquist. Nucleated conformational conversion and the replication of conformational information by a prion determinant. *Science*, 289(5483):1317–1321, 2000.

[124] Diego O Serra, Anja M Richter, Gisela Klauck, Franziska Mika, and Regine Hengge. Microanatomy at cellular resolution and spatial order of physiological differentiation in a bacterial biofilm. *MBio*, 4(2):e00103–13, 2013.

[125] Frank Shewmaker, Ryan P McGlinchey, Kent R Thurber, Peter McPhie, Fred Dyda, Robert Tycko, and Reed B Wickner. The functional curli amyloid is not based on in-register parallel β-sheet structure. *Journal of Biological Chemistry*, 284(37):25065–25076, 2009.

[126] Mike Sleutel, Imke Van den Broeck, Nani Van Gerven, Cécile Feuillie, Wim Jonckheere, Claire Valotteau, Yves F Dufrêne, and Han Remaut. Nucleation and growth of a bacterial functional amyloid at single-fiber resolution. *Nature chemical biology*, 13(8):902, 2017.

[127] Ethan B Solomon, Brendan A Niemira, Gerald M Sapers, and Bassam A Annous. Biofilm formation, cellulose production, and curli biosynthesis by salmonella originating from produce, animal, and clinical sources. *Journal of food protection*, 68(5):906–912, 2005.

[128] Olga Soutourina, Olivier Poupel, Jean-Yves Coppée, Antoine Danchin, Tarek Msadek, and Isabelle Martin-Verstraete. Cymr, the master regulator of cysteine metabolism in staphylococcus aureus, controls host sulphur source utilization and plays a role in biofilm formation. *Molecular microbiology*, 73(2):194–211, 2009.

[129] Walter E Stamm. Scientific and clinical challenges in the management of urinary tract infections. *The American journal of medicine*, 113(1):1–4, 2002.

[130] Joan S Steffan, Aleksey Kazantsev, Olivera Spasic-Boskovic, Marilee Greenwald, Ya-Zhen Zhu, Heike Gohler, Erich E Wanker, Gillian P Bates, David E Housman, and Leslie M Thompson. The huntington's disease protein interacts with p53 and creb-binding protein and represses transcription. *Proceedings of the National Academy of Sciences*, 97(12):6763–6768, 2000.

[131] Gwen Sturgill, Christine M Toutain, John Komperda, George A O'toole, and Philip N Rather. Role of cyse in production of an extracellular signaling molecule in providencia stuartii and escherichia coli: loss of cyse enhances biofilm formation in escherichia coli. *Journal of bacteriology*, 186(22):7610–7617, 2004.

[132] Margaret Sunde and Colin Blake. The structure of amyloid fibrils by electron microscopy and x-ray diffraction. In *Advances in protein chemistry*, volume 50, pages 123–159. Elsevier, 1997.

[133] Jonathan D Taylor, William J Hawthorne, Joanne Lo, Alexander Dear, Neha Jain, Georg Meisl, Maria Andreasen, Catherine Fletcher, Marion Koch, Nicholas Darvill, et al. Electrostatically-guided inhibition of curli amyloid nucleation by the csgc-like family of chaperones. *Scientific reports*, 6:24656, 2016.

[134] Jonathan D Taylor, Yizhou Zhou, Paula S Salgado, Ardan Patwardhan, Matt McGuffie, Tillmann Pape, Grzegorz Grabe, Elisabeth Ashman, Sean C Constable, Peter J Simpson, et al. Atomic resolution insights into curli fiber biogenesis. *Structure*, 19(9):1307–1316, 2011.

[135] Pengfei Tian, Wouter Boomsma, Yong Wang, Daniel E Otzen, Mogens H Jensen, and Kresten Lindorff-Larsen. Structure of a functional amyloid protein subunit computed using sequence variation. *Journal of the American Chemical Society*, 137(1):22–25, 2014.

[136] Heather L True and Susan L Lindquist. A yeast prion provides a mechanism for genetic variation and phenotypic diversity. *Nature*, 407(6803):477, 2000.

[137] Çagla Tükel, Jessalyn H Nishimori, R Paul Wilson, Maria G Winter, A Marijke Keestra, Jos PM Van Putten, and Andreas J Bäumler. Toll-like receptors 1 and 2 cooperatively mediate immune responses to curli, a common amyloid from enterobacterial biofilms. *Cellular microbiology*, 12(10):1495–1505, 2010.

[138] Çagla Tükel, Manuela Raffatellu, Andrea D Humphries, R Paul Wilson, Helene L Andrews-Polymenis, Tamara Gull, Josely F Figueiredo, Michelle H Wong, Kathrin S Michelsen, Mustafa Akçelik, et al. Csga is a pathogen-associated molecular pattern of salmonella enterica serotype typhimurium that is recognized by toll-like receptor 2. *Molecular microbiology*, 58(1):289–304, 2005.

[139] Sarah A Tursi, Ernest Y Lee, Nicole J Medeiros, Michael H Lee, Lauren K Nicastro, Bettina Buttaro, Stefania Gallucci, Ronald Paul Wilson, Gerard CL Wong, and Çagla Tükel. Bacterial amyloid curli acts as a carrier for dna to elicit an autoimmune response via tlr2 and tlr9. *PLoS pathogens*, 13(4):e1006315, 2017.

[140] Jaione Valle, Sandra Da Re, Nelly Henry, Thierry Fontaine, Damien Balestrino, Patricia Latour-Lambert, and Jean-Marc Ghigo. Broad-spectrum biofilm inhibition by a secreted bacterial polysaccharide. *Proceedings of the National Academy of Sciences*, 103(33):12558–12563, 2006.

[141] Nani Van Gerven, Roger D Klein, Scott J Hultgren, and Han Remaut. Bacterial amyloid formation: structural insights into curli biogensis. *Trends in microbiology*, 23(11):693–706, 2015.

[142] Martijn E van Raaij, Ine MJ Segers-Nolten, and Vinod Subramaniam. Quantitative morphological analysis reveals ultrastructural diversity of amyloid fibrils from α-synuclein mutants. *Biophysical journal*, 91(11):L96–L98, 2006.

[143] Kostas Vekrellis, Maria Xilouri, Evangelia Emmanouilidou, Hardy J Rideout, and Leonidas Stefanis. Pathological roles of α-synuclein in neurological disorders. *The Lancet Neurology*, 10(11):1015–1025, 2011.

[144] Olivier Vidal, Robert Longin, Claire Prigent-Combaret, Corinne Dorel, Michel Hooreman, and Philippe Lejeune. Isolation of an escherichia coli k-12 mutant strain able to form biofilms on inert surfaces: involvement of a new ompr allele that increases curli expression. *Journal of bacteriology*, 180(9):2442–2449, 1998.

[145] Helen E Vuong, Jessica M Yano, Thomas C Fung, and Elaine Y Hsiao. The microbiome and host behavior. *Annual review of neuroscience*, 40:21–49, 2017.

[146] Dandan Wang, Xuedong Ding, and Philip N Rather. Indole can act as an extracellular signal inescherichia coli. *Journal of Bacteriology*, 183(14):4210–4216, 2001.

[147] Xuan Wang. The determinants of bacterial amyloid nucleation and polymerization. 2008.

[148] Xuan Wang, Daniel R Smith, Jonathan W Jones, and Matthew R Chapman. In vitro polymerization of a functional escherichia coli amyloid protein. *Journal of Biological Chemistry*, 282(6):3713–3719, 2007.

[149] Xuan Wang, Yizhou Zhou, Juan-Jie Ren, Neal D Hammer, and Matthew R Chapman. Gatekeeper residues in the major curlin subunit modulate bacterial amyloid fiber biogenesis. *Proceedings of the National Academy of Sciences*, 107(1):163–168, 2010.

[150] Harald Weber, Christina Pesavento, Alexandra Possling, Gilbert Tischendorf, and Regine Hengge. Cyclic-di-gmp-mediated signalling within the σs network of escherichia coli. *Molecular microbiology*, 62(4):1014–1034, 2006.

[151] Michal Weiss-Muszkat, Dana Shakh, Yizhou Zhou, Riky Pinto, Eddy Belausov, Matthew R Chapman, and Shlomo Sela. Biofilm formation by and multicellular behavior of escherichia coli o55: H7, an atypical enteropathogenic strain. *Appl. Environ. Microbiol.*, 76(5):1545–1554, 2010.

[152] Benjamin G Wilhelm, Sunit Mandad, Sven Truckenbrodt, Katharina Kröhnert, Christina Schäfer, Burkhard Rammner, Seong Joo Koo, Gala A Claßen, Michael Krauss, Volker Haucke, et al. Composition of isolated synaptic boutons reveals the amounts of vesicle trafficking proteins. *Science*, 344(6187):1023–1028, 2014.

[153] Stephen J Wood, Jette Wypych, Shirley Steavenson, Jean-Claude Louis, Martin Citron, and Anja Leona Biere. α-synuclein fibrillogenesis is nucleation-dependent implications for the pathogenesis of parkinson s disease. *Journal of Biological Chemistry*, 274(28):19509–19512, 1999.

[154] Michael M Wördehoff, Oliver Bannach, Hamed Shaykhalishahi, Andreas Kulawik, Stephanie Schiefer, Dieter Willbold, Wolfgang Hoyer, and Eva Birkmann. Single fibril growth kinetics of α-synuclein. *Journal of molecular biology*, 427(6):1428–1435, 2015.

[155] Kelly J Wright, Patrick C Seed, and Scott J Hultgren. Development of intracellular bacterial communities of uropathogenic escherichia coli depends on type 1 pili. *Cellular microbiology*, 9(9):2230–2241, 2007.

[156] Xiaoqian Wu, Yu Wang, and Liang Tao. Sulfhydryl compounds reduce staphylococcus aureus biofilm formation by inhibiting pia biosynthesis. *FEMS microbiology letters*, 316(1):44–50, 2011.

[157] Laurence J Young, Gabriele S Kaminski Schierle, and Clemens F Kaminski. Imaging aβ (1–42) fibril elongation reveals strongly polarised growth and growth incompetent states. *Physical Chemistry Chemical Physics*, 19(41):27987–27996, 2017.

[158] Chunhui Zhao, Yoichi Kumada, Hiroyuki Imanaka, Koreyoshi Imamura, and Kazuhiro Nakanishi. Cloning, overexpression, purification, and characterization of o-acetylserine sulfhydrylase-b from escherichia coli. *Protein expression and purification*, 47(2):607–613, 2006.

[159] Yizhou Zhou, Daniel Smith, Bryan J Leong, Kristoffer Brännström, Fredrik Almqvist, and Matthew R Chapman. Promiscuous cross-seeding between bacterial amyloids promotes interspecies biofilms. *Journal of Biological Chemistry*, 287(42):35092–35103, 2012.

[160] Yizhou Zhou, Daniel R Smith, David A Hufnagel, and Matthew R Chapman. Experimental manipulation of the microbial functional amyloid called curli. In *Bacterial cell surfaces*, pages 53–75. Springer, 2013.

[161] Jun Zhu and John J Mekalanos. Quorum sensing-dependent biofilms enhance colonization in vibrio cholerae. *Developmental cell*, 5(4):647–656, 2003.

[162] Xhavit Zogaj, Werner Bokranz, Manfred Nimtz, and Ute Römling. Production of cellulose and curli fimbriae by members of the family enterobacteriaceae isolated from the human gastrointestinal tract. *Infection and immunity*, 71(7):4151–4158, 2003.

[163] Xhavit Zogaj, Manfred Nimtz, Manfred Rohde, Werner Bokranz, and Ute Römling. The multicellular morphotypes of salmonella typhimurium and escherichia coli produce cellulose as the second component of the extracellular matrix. *Molecular microbiology*, 39(6):1452–1463, 2001.

CHAPTER V

Appendix

5.1 Chapter 2 – Supplementary figures

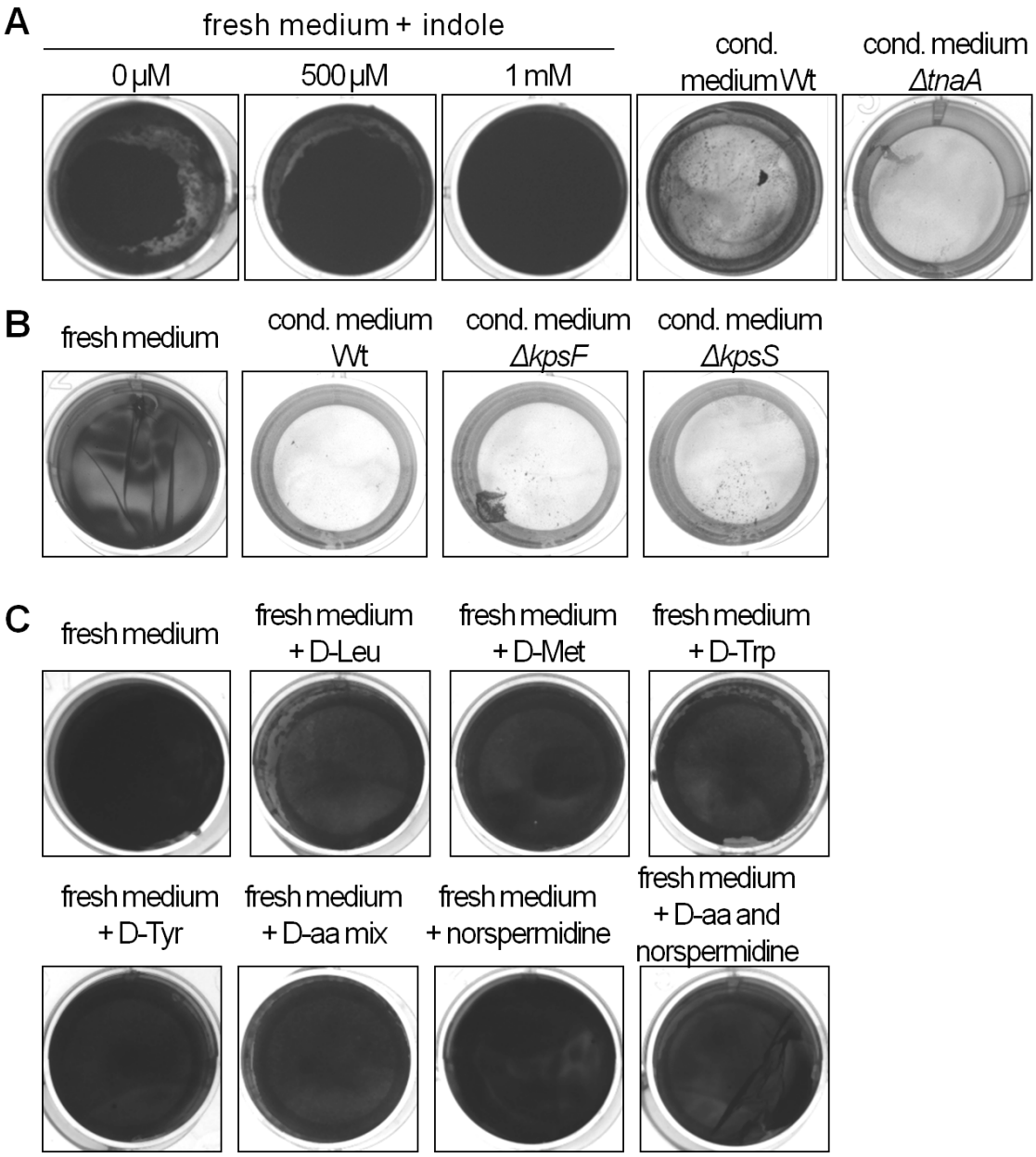

Figure 5.1: The antibiofilm activity was not due to reported biofilm inhibitors including indole, capsular polysaccharides, D-amino acids and norspermidine. (A) UTI89 grown at 26°C for 48 hours in fresh YESCA medium added with 0 μM, 500 μM, or 1 mM indole, or conditioned medium from 4 day old cultures of wild-type UTI89 or a δtnaA mutant. **(B)** UTI89 grown at 26°C for 48 hours in the fresh medium, or conditioned media collected from 4 day old cultures of wild-type, ΔkpsF mutant or δkpsS mutant. **(C)** UTI89 grown at 26°C for 48 hour in fresh medium, or fresh medium supplemented with 1 mM D-Leucine, 1 mM D-Methionine, 1 mM D-Tryptophan, 1 mM D-Tyrosine or 1 mM D-amino acid mix (D-Leu, D-Met, D-Try, D-Tyr), 100 μM norspermidine, or a combination of 100 μM D-amino acids and 100 μM norspermidine. Bacteria were grown in wells on 24 well tissue culture plates, and each well was stained with crystal violet for better visualization.

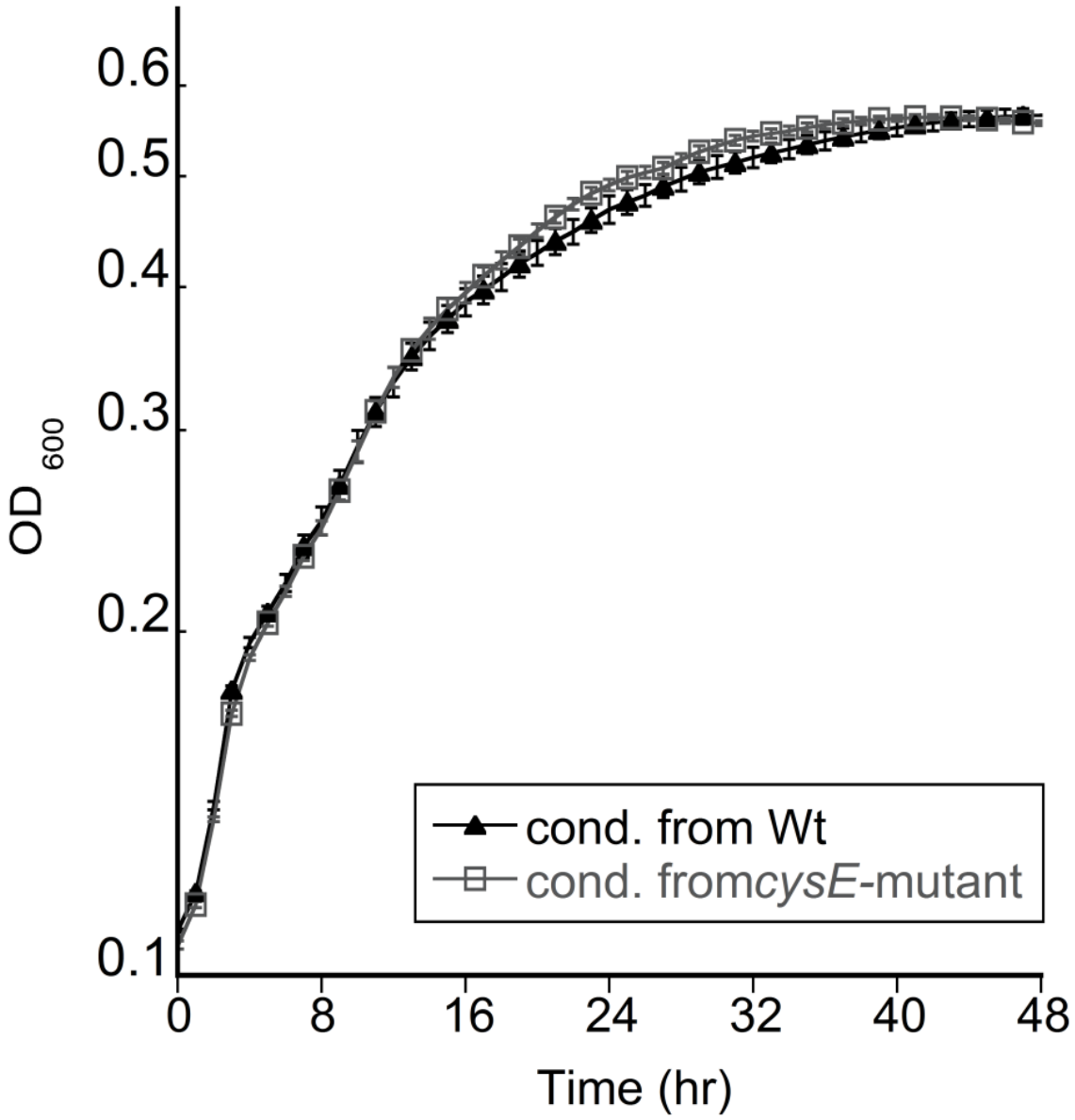

Figure 5.2: Growth curves of UTI89 grown in the conditioned medium collected from 4 day old cultures of wild-type or a δcysE mutant. Optical density was measured at 600 nm by plate reader. Each data point represents the average of 6 replicates.

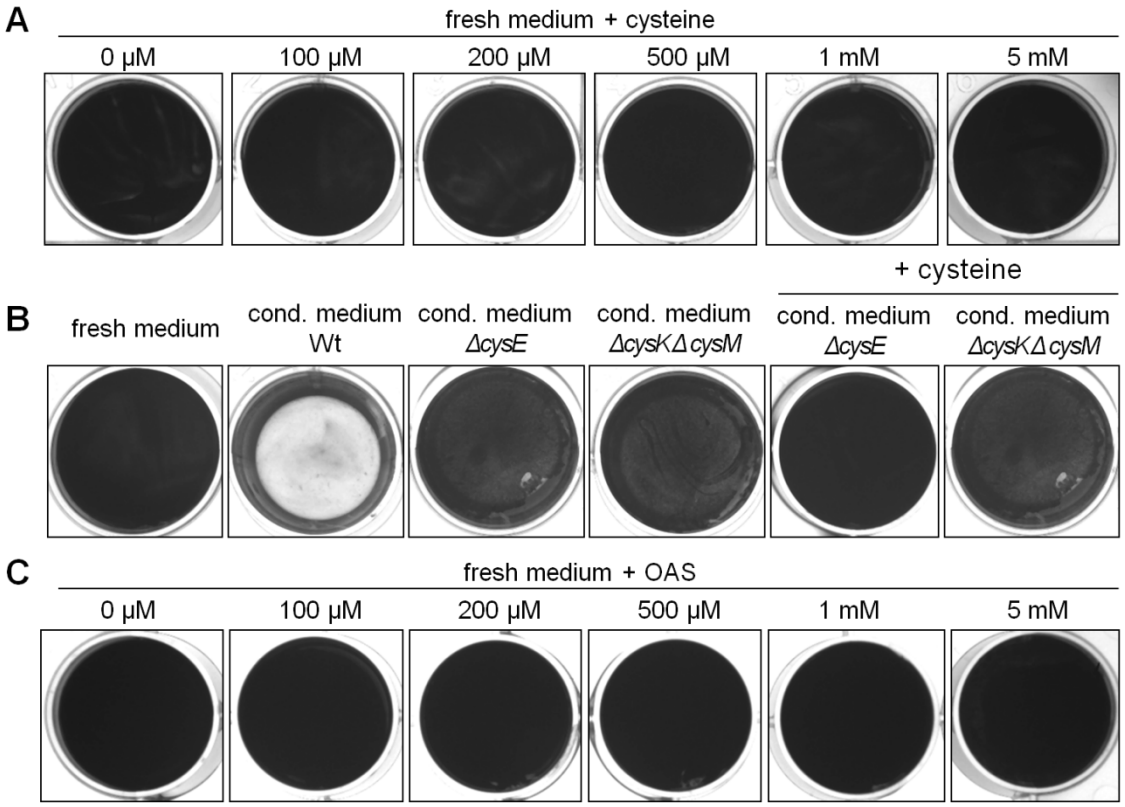

Figure 5.3: Cysteine did not directly inhibit pellicle formation. (A) UTI89 was grown in fresh medium supplemented with 100 μM or 1 mM cysteine at 26°C for 48 hoursr. (B) UTI89 was grown at 26°C for 48 hours in fresh medium, wild-type conditioned medium, δcysE conditioned medium, δcysKδcysM conditioned medium, or δcysE and δcysKδcysM conditioned media post-supplemented with 100 μM cysteine. Wells were stained with crystal violet.

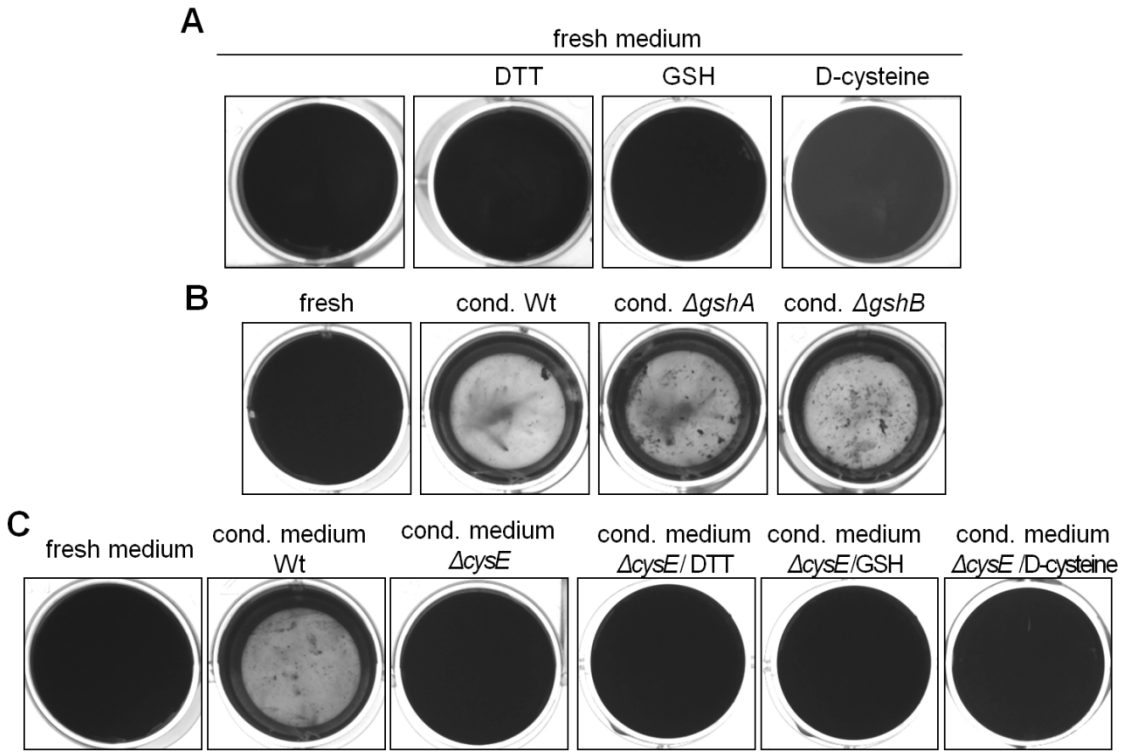

Figure 5.4: DTT, glutathione (GSH) or D-cysteine did not contribute to the antibiofilm activity of the conditioned medium. (A) UTI89 grown at 26°C for 48 hours in fresh medium in the presence of 1 mM DTT, GSH or D-cysteine. **(B)** UTI89 grown in fresh medium or conditioned media collected from 4 day old cultures of wild-type, δgshA or δgshB. **(C)** UTI89 grown in fresh medium, conditioned media from wild-type or δcysE cultures, or conditioned media from δcysE cultures supplemented with GSH or D-cysteine.